

NAVAL POSTGRADUATE SCHOOL

Monterey, California



THESIS

AMPLITUDE SHADING AND PHASE WEIGHTING OF A
VERTICAL LINEAR ARRAY IN THE SOFAR CHANNEL
BY THE LINEAR MINIMUM VARIANCE
ESTIMATION TECHNIQUE

by

Daniel Patrick McVicar

December 1983

Thesis Advisor:

P. H. Moose

Approved for public release; distribution unlimited

T215648

REPORT DOCUMENTATION PAGE		READ INSTRUCTIONS BEFORE COMPLETING FORM
1. REPORT NUMBER	2. GOVT ACCESSION NO.	3. RECIPIENT'S CATALOG NUMBER
4. TITLE (and Subtitle) Amplitude Shading and Phase Weighting of a Vertical Linear Array in the SOFAR Channel by the Linear Minimum Variance Estimation Technique		5. TYPE OF REPORT & PERIOD COVERED Master's Thesis December 1983
		6. PERFORMING ORG. REPORT NUMBER
7. AUTHOR(s) Daniel Patrick McVicar		8. CONTRACT OR GRANT NUMBER(s)
9. PERFORMING ORGANIZATION NAME AND ADDRESS Naval Postgraduate School Monterey, California 93943		10. PROGRAM ELEMENT, PROJECT, TASK AREA & WORK UNIT NUMBERS
11. CONTROLLING OFFICE NAME AND ADDRESS Naval Postgraduate School Monterey, California 93943		12. REPORT DATE December 1983
		13. NUMBER OF PAGES 90
14. MONITORING AGENCY NAME & ADDRESS (if different from Controlling Office)		15. SECURITY CLASS. (of this report)
		15a. DECLASSIFICATION/DOWNGRADING SCHEDULE
16. DISTRIBUTION STATEMENT (of this Report) Approved for public release; distribution unlimited		
17. DISTRIBUTION STATEMENT (of the abstract entered in Block 20, if different from Report)		
18. SUPPLEMENTARY NOTES		
19. KEY WORDS (Continue on reverse side if necessary and identify by block number) Linear Minimum Variance Estimation Depth Estimation Vertical Linear Array SOFAR Channel		
20. ABSTRACT (Continue on reverse side if necessary and identify by block number) A single linear vertical passive array is used in the 'SOFAR' channel to determine the depth of a single underwater source at a constant range. The phase and amplitude weights applied to the array are determined by the linear minimum variance estimation technique. The resulting beam pattern is compared to the conventional time domain beamformer. It was found that the linear minimum variance estimation technique of amplitude shading and phase weighting was significantly superior to the conventional beamformer.		

Approved for public release; distribution unlimited.

Amplitude Shading and Phase Weighting of a Vertical Linear Array
in the SOFAR Channel
by the Linear Minimum Variance Estimation Technique

by

Daniel P. McVicar
Captain, Canadian Armed Forces
B.Eng., Nova Scotia Technical College, 1976

Submitted in partial fulfillment of the
requirements for the degrees of
MASTER OF SCIENCE IN ENGINEERING ACOUSTICS
and
MASTER OF SCIENCE IN ELECTRICAL ENGINEERING
from the

NAVAL POSTGRADUATE SCHOOL
December 1983

ABSTRACT

A single linear vertical passive array is used in the 'SOFAR' channel to determine the depth of a single underwater source at a constant range. The phase and amplitude weights applied to the array are determined by the linear minimum variance estimation technique. The resulting beam pattern is compared to the conventional time domain beamformer. It was found that the linear minimum variance estimation technique of amplitude shading and phase weighting was significantly superior to the conventional beamformer.

TABLE OF CONTENTS

I.	INTRODUCTION	9
II.	GENERAL THEORY	13
	A. RAY ACOUSTICS	13
	B. ARRAY MODEL	18
	C. LINEAR MINIMUM VARIANCE METHOD	23
III.	EXPERIMENTAL PROCEDURE	32
	A. BASIC ASSUMPTIONS	32
	B. ' <u>A</u> ' MATRIX CALCULATION	32
	C. ' <u>Z</u> ' MATRIX	34
	D. RESULTING BEAM PATTERN	34
	1. Using the Linear Minimum Variance Method	34
	2. Using Linear Phase Shifts	35
IV.	RESULTS	40
	A. EXACT SOLUTION	40
	B. FOUR DEPTHS WITH TWO RECEIVERS	40
	C. TWENTY DEPTHS WITH TWO RECEIVERS	40
	D. TWENTY DEPTHS WITH FIVE RECEIVERS	41
	E. CONVENTIONAL BEAMFORMER	41
	F. RANGE OF 250 KILOMETERS	42
V.	DISCUSSION OF RESULTS AND RECOMMENDATIONS	66
	APPENDIX A: RELATIVE TRAVEL TIME CALCULATION	68
	APPENDIX E: INTERPOLATION OF RELATIVE TRAVEL TIME CALCULATIONS	81

APPENDIX C: RESULTING BEAM PATTERN FOR CALCULATED	
WEIGHTS	84
LIST OF REFERENCES	89
INITIAL DISTRIBUTION LIST	90

LIST OF TABLES

I.	Relative Travel Times For 380 Meter Source	
	Depth	36
II.	Slower Ray Travel Times For 250 km Range and	
	380 m Source	43
III.	Faster Travel Times For 250 km Range and 380 m	
	Source	43

LIST OF FIGURES

2.1	Circular Ray Path	15
2.2	Single Ray Path Plot In Triangular SOFAR Channel	29
2.3	Ray Plot For Assumed Sound Channel	30
2.4	Array Model	31
3.1	Relative Travel Time vs. Depth (220 meter source)	37
3.2	Relative Travel Time vs. Depth (380 meter source)	38
3.3	Straight Line Approx. of Rel. Trav. Time vs. Depth (source at 380 m)	39
4.1	Beam Amplitude vs. Source Depth (5 depths 5 receivers)	44
4.2	Beam Pattern (4 depths 2 receivers, source at 220 m)	45
4.3	Beam Pattern (4 depths 2 receivers, source at 280 m)	46
4.4	Beam Pattern (20 depths 2 receivers, source at 220 m)	47
4.5	Beam Pattern (20 depths 2 receivers, source at 380 m)	48
4.6	Beam Pattern (20 depths 5 receivers, source at 220 m)	49
4.7	Beam Pattern (20 depths 5 receivers, source at 360 m)	50
4.8	Beam Pattern (20 depths 5 receivers, source at 380 m)	51
4.9	Beam Pattern (20 depths 5 receivers, source at 400 m)	52

4.10	Conventional Beam Pattern (source at 380 meters)	53
4.11	Conventional Beam Pattern (non-unity amp. wts. source at 380 m)	54
4.12	Relative Travel Time vs. Depth (range=250 km, source at 220 m)	55
4.13	Relative Travel Time vs. Depth (range=250 km, source at 380 m)	56
4.14	St. Line Approx. of Rel. Trav. Time vs. Depth (R=250 km, d=380 m)	57
4.15	Conventional Beam Pattern (R=250 km, d=380 m, slower times, a=1)	58
4.16	Conventional Beam Pattern (R=250 km, d=380 m, slower times, LMV a)	59
4.17	Conventional Beam Pattern (R=250 km, d=380 m, faster times, a=1)	60
4.18	Conventional Beam Pattern (R=250 km, d=380 m, faster times, LMV a)	61
4.19	Beam Pattern (R=250 km, 20 depths, 5 receivers, source at 220 m)	62
4.20	Beam Pattern (R=250 km, 20 depths, 5 receivers, source at 340 m)	63
4.21	Beam Pattern (R=250 km, 20 depths, 5 receivers, source at 360 m)	64
4.22	Beam Pattern (R=250 km, 20 depths, 5 receivers, source at 380 m)	65

I. INTRODUCTION

There are many solutions to the problem of predicting the location of an underwater energy source. One common solution is the use of a passive hydrophone which detects the pressure waves radiating from the source. The hydrophone sensor is assumed to be omnidirectional and therefore incapable of estimating direction. To provide directionality a series of sensors are placed in a row to form a passive linear array.

A familiar method of determining directionality is time-domain beamforming. In this principle, it is assumed that the source is far enough away so that the pressure wave appears to be a plane wave when viewed at the site of the receiving array.

Thus a set of time delays are calculated for any direction of signal arrival, which, when applied to the receiver outputs causes them to be in phase and to reinforce when summed. The resultant angular response to signals arriving from other than the nominated direction is then a function of the array geometry, relative to the signal wavelength, and any weighting factors which have been applied to the receiver outputs. The effect is to generate a main receiving beam in the desired direction, with a series of undesired subsidiary sidelobes whose magnitude can be controlled to some extent by the choice of a suitable array geometry and the use of amplitude weightings on the receiver outputs.

In order to determine location, three or more such arrays separated by a known amount may be used.

This study is concerned with a single linear vertical passive array and the determination of the depth of a single

underwater source. The analysis is based on the following assumptions:

- The underwater source is emitting continuously and at a monochromatic frequency.
- Both the source and receiving hydrophones are stationary in space causing a constant range.
- The range is sufficiently long so that the channel is filled with R-R (refracted-refracted) rays.
- There is no distortion introduced in the propagating medium so that the signals received at each sensor are identical except for constant delays.
- The source signal and noise are independent and stationary gaussian random processes.
- The speed of sound profile is triangular and symmetric with the deep sound channel axis at 1000 meters. The velocity gradient is -0.017 meters/meter/sec above 1000 meters and $+0.017$ meters/meter/sec below 1000 meters. This profile gives a speed of sound at the surface of 1500 meters/sec.
- The speed of sound profile is constant in the horizontal plane.
- Only R-R rays are considered. All other rays have sufficient loss that their effect is negligible.

As opposed to conventional time-domain beamforming, this study makes no assumption of planar wave fronts at the receiver site. Therefore the time delays applied to each receiver will not, in general, be a linear function of depth.

Since it is desired to determine whether or not there is a source present at a specific depth the result will be a

binary decision. A "1" will indicate signal source present; a "0" will indicate signal source not present. For the constant range there will be "N" test depths investigated for the signal source. The number of hydrophones in the vertical array will be "L".

For a single source at a given depth, the travel time is calculated from the depth to each hydrophone. This travel time is converted into a phase delay for each hydrophone so that after summation from all hydrophones a maximum output is achieved. This output is then passed through a squaring device, an integrator, and a threshold and flip flop device to give a "1" binary output. If the signal source is at a different depth and the same previous phase delays are used for each hydrophone then the output will be somewhat less than the previous maximum. The difference in depth required to achieve a "0" binary output is the depth resolution of the system.

The travel times for each hydrophone are calculated for each of the "N" source depths to be considered. "N" will ordinarily be much greater than "L" so that the system will be overdetermined. An overdetermined system is one in which there are more equations than unknowns. The objective then is to calculate the phase angle and amplitude weight for each hydrophone so that a determination can be made indicating the presence or absence of a signal source at a given depth.

The method used to calculate the phase and amplitude weights is the linear minimum variance estimation technique. Linear minimum variance estimators are optimum when compared with all other estimators for gaussian problems. The method is directly applicable to overdetermined systems.

The output of the summer is calculated using the linear minimum variance amplitude and phase angles assuming a source at one of the "N" source depths and no source at the

others. The calculation is repeated for each of the depths. The result, when plotted against source depth, will be referred to as the "beam pattern" of the array in this report. (Although similar, it should not be interpreted as the angular response of an array as in the conventional definition of a beam pattern. The conventional definition loses much of its utility when the wavefronts are not planar.) Ideally the beam pattern will be maximum at the desired depth and very small at all other depths so that the binary "1" decision will be made for a source at the desired depth, and a "0" decision for sources at all others. This beam pattern is compared with the depth beam pattern of the conventional time-domain beamformer mentioned above. The purpose of this thesis is to determine, as an initial investigation, whether the linear minimum variance estimation technique, when applied to a linear vertical array, is useful in depth discrimination at long ranges in a 'SOFAR' type sound channel.

II. GENERAL THEORY

A. RAY ACOUSTICS

The propagation of sound in an elastic medium can be described mathematically by solutions of the wave equation using the appropriate boundary and medium conditions for a particular problem. The wave equation relating the acoustic pressure 'p' to the coordinates 'x', 'y', 'z', and the time 't', may be written as

$$\frac{d^2 p}{dt^2} = c^2 \left(\frac{d^2 p}{dx^2} + \frac{d^2 p}{dy^2} + \frac{d^2 p}{dz^2} \right) \quad (2.1)$$

where 'c' is a quantity that has the general significance of sound velocity and may vary with the coordinates.

One may approximate the solution of the wave equation using ray theory: its body of results and conclusions is called ray acoustics.

Officer [Ref. 1] describes the ray solution as a complete solution to any particular propagation problem within the validity of the approximation of the Eikonal equation to the wave equation. For these approximations to be valid neither the amplitude of the wave nor the speed of sound can change appreciably in distances comparable to a wavelength.

Thus the path of a ray through a medium in which the speed of sound varies with depth can be calculated by the application of Snell's law

$$\cos\theta/c = 1/c_0 = \text{a constant for any one ray} \quad (2.2)$$

where ' θ ' is the angle of depression made with the horizontal at a depth where the speed of sound is ' c ', and ' c_0 ' is the speed at a depth (real or extrapolated) where the ray would become horizontal.

In a medium in which the velocity of sound changes linearly with depth the sound rays can be shown to be arcs of circles, that is, to have a constant radius of curvature. Kinsler et al. [Ref. 2] give a simple and heuristic demonstration of the circularity of rays in a medium with a linear sound speed gradient ' g '. The center of the circle which creates the arc lies at a depth where the sound speed extrapolates to zero. To understand this, consider a portion of a ray path with a local radius of curvature ' R ', as illustrated in Figure 2.1. Since the gradient ' g ' for this case is

$$g = \Delta c / \Delta z = (c_2 - c_1) / (d_2 - d_1) = (c_2 - c_1) / R (\cos \theta_1 - \cos \theta_2) \quad (2.3)$$

where ' Δc ' is the change in sound speed and ' Δz ' is the change in depth. It can be seen that the radius of curvature is given by

$$R = -c_0 / g = -c / (g \cos \theta) \quad (2.4)$$

The ray path is therefore a circle when ' g ' is constant because ' R ' is then constant. The center of curvature of a circle lies at the depth where θ is 90 degrees, which corresponds to $c=0$. For the situation in Figure 2.1 the speed gradient is negative so that ' R ' is positive. If the speed gradient were positive ' R ' would be negative, and the path would curve upward.

Once the radius of curvature of each segment of a path is known the actual path can be traced graphically or

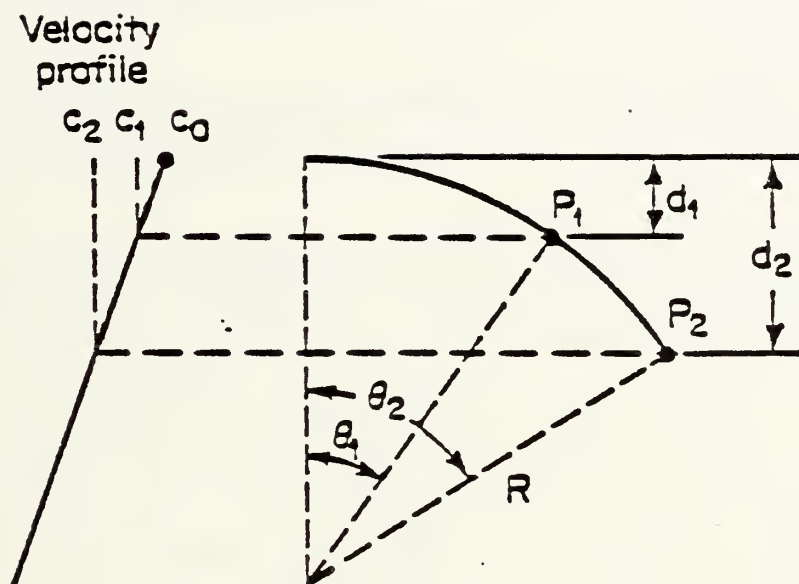


Figure 2.1 Circular Ray Path

computed. If the initial angle of depression of a ray is θ_1 , then by referring to the geometry of Figure 2.1 the changes in both range and depth are

$$\Delta r = c_1 (\sin(\theta_1) - \sin(\theta_2)) / (g \cos(\theta_1)) \quad (2.5)$$

$$\Delta z = c_1 (\cos(\theta_2) - \cos(\theta_1)) / (g \cos(\theta_1)) \quad (2.6)$$

The sign convention for these equations is: downward, to the right, and depression angles below the horizontal axis positive.

The symmetric triangular sound speed profile assumed in the introduction is similar to speed profiles encountered in the deep sound channel, sometimes called the SOFAR channel. The velocity minimum which occurs at the axis of the sound channel causes the sea to act like a kind of lens; above and below the minimum, the velocity gradient continually bends the sound rays toward the depth of minimum velocity. A portion of the power radiated by a source in the deep sound channel accordingly remains within the channel and encounters no acoustic losses by reflection from the surface and bottom. These rays are called R-R (refracted-refracted) and since they have very low transmission loss, very long ranges can be obtained from a source of moderate acoustic power output. Thus an energy source at a specific depth will propagate energy in all directions but only the direction which is toward the receiving array and for which the rays are R-R is of interest. To determine the range of depression angles which will yield R-R rays Snell's law is used to give

$$\theta_{\max} = \arccos (c_1 / (c_1 - (g \ d))) \quad (2.7)$$

where ' θ_{\max} ' is in radians and ' c_1 ' is the speed of sound at the source depth ' d '.

An example is given in Figure 2.2 of a single ray trace propagating in the SOFAR channel to show how equations 2.5 and 2.6 are used in determining range and depth. The ray path is broken up into arcs of circles as shown in the figure, and then by paying close attention to the previously defined sign conventions, the change in range and depth is found. Being more specific, for arc 1, θ_1 and θ_2 are both positive; for arc 2, θ_1 is positive and θ_2 is zero; for arc 3, θ_1 is zero and θ_2 is negative; and for arc 4, θ_1 is negative and θ_2 is zero. By keeping a running total of all the depth and range changes it is possible to determine the total horizontal distance travelled and the depth at that distance.

For the speed of sound profile assumed in the introduction a computer generated ray plot is shown in Figure 2.3 for a source depth of 300 meters. As each ray propagates out from the source the triangular channel becomes filled with sound. If a receiving hydrophone is placed a great distance away, a number of refracted propagation paths will exist, each having a different travel time and crossing the channel axis at different intervals. The path with the greatest excursion from the axis will have the shortest travel time.

Officer [Ref. 1] shows that the travel time ' t ' of a ray, which is an arc of a circle, is given by

$$t = \frac{1}{g} \int_{\theta_1}^{\theta_2} \frac{d\theta}{\cos \theta} \quad (2.8)$$

and the travel time for each arc is

$$t = - \frac{1}{g} \log_e \left[\frac{\tan((\pi/4) + (\theta_2/2))}{\tan((\pi/4) + (\theta_1/2))} \right] \quad (2.9)$$

Equation 2.9, applied using the same convention as equations 2.5 and 2.6, determines the total travel time of a ray in the deep sound channel.

B. ARRAY MODEL

The receiving linear vertical array is presumed to consist of 'L' hydrophones as shown in Figure 2.4. It is assumed that the source is emitting energy at a constant frequency, 'f', and amplitude, 'A', regardless of the depth. The source signal at the source is $A \exp(j2\pi ft)$. The inherent received signal at the first hydrophone is

$$x_1(t) = A \exp(j2\pi f(t-t_1)) \quad (2.10)$$

where 't₁' is the travel time from the energy source to the first hydrophone and 'A' is the amplitude of the signal at the range of the array. After passage through the amplitude weight 'a₁' and a phase delay of 'τ₁', the signal on the first hydrophone at the input to the summer is

$$y_1(t) = A a_1 x_1(t - \tau_1) = A a_1 \exp(j2\pi f(t - t_1 - \tau_1)) \quad (2.11)$$

A time delay, for monochromatic signals corresponds to a phase shift

$$\theta = 2\pi f t \quad (2.12)$$

where 'θ' is the phase shift in radians and 't' is the time delay in seconds. Thus equation 2.11 can be written as

$$y_1(t) = A' a_1 \exp(j(2\pi ft - \phi_1 - \theta_1)) \quad (2.13)$$

where ' $\phi_1 = 2\pi ft_1$ ' is the phase delay due to the travel time from the source to the first hydrophone and ' θ_1 ' is the phase delay in the receiver on the first hydrophone.

Combining all the hydrophones in the array in a summer gives as an expression for the array output

$$Y(t) = \sum_{k=1}^L A' a_k \exp(j(2\pi ft - \phi_k - \theta_k)) \quad (2.14)$$

where ' ϕ_k ' represents the phase delay due to the travel time from the source to the "k th" hydrophone and ' θ_k ' is the phase delay in the receiver on the "k th" hydrophone. If the amplitude of the energy source is normalized by setting $A'=1$, and equation 2.14 is written in terms of real and imaginary components, we have

$$Y(t) = \sum_{k=1}^L a_k \cos(-\phi_k - \theta_k) + j \sin(-\phi_k - \theta_k) \exp(j2\pi ft) \quad (2.15)$$

When an energy source is at the "q th" depth, we wish to have each receiving hydrophone's phase delay cancel out the effect of the travel time from the source to it, such that ' $-\phi_k - \theta_k$ ' is equal to a multiple of ' 2π '. This will put all signals into the summer in phase and thus maximize the signal gain for a source at the "q th" depth. From equation 2.15,

$$\sum_{k=1}^L (a_{kq} \cos(-\phi_{kq} - \theta_{kq})) = L \quad (\text{source present at } q) \quad (2.16)$$

$$\sum_{k=1}^L (a_{kq} \sin(-\phi_{kq} - \theta_{kq})) = 0 \quad (\text{source present at } q) \quad (2.17)$$

Note that the first subscript on the phase angle indicates the receiving hydrophone and the second subscript indicates the depth of the source. Thus ' ϕ_{kq} ' would indicate the phase shift relating to the travel time from the "q th" test depth to the "k th" hydrophone in the receiving array.

It is desirable for ' $Y(t)$ ' to be a minimum value for sources at other than the depth being investigated. Thus for each of the other ' $N-1$ ' depths ' $Y(t)$ ' is set to zero. This gives ' $N-1$ ' equations for the real terms of ' $Y(t)$ ' set to zero

$$\sum_{k=1}^L a_{kq} \cos(-\phi_{km} - \theta_{kq}) = 0 \quad (\text{source absent; } m \neq q) \quad (2.18)$$

and ' $N-1$ ' equations for the imaginary terms of ' $Y(t)$ ' set to zero

$$\sum_{k=1}^L a_{kq} \sin(-\phi_{km} - \theta_{kq}) = 0 \quad (\text{source absent; } m \neq q) \quad (2.19)$$

By using elementary trigonometric identities, equation 2.16 (real terms with source present at "q th" depth) becomes

$$\sum_{k=1}^L a_{kq} [\cos(\phi_{kq}) \cos(\theta_{kq}) - \sin(\phi_{kq}) \sin(\theta_{kq})] = L \quad (2.20)$$

Equation 2.18 (real terms with source absent for each of the other ' $N-1$ ' depths) becomes

$$\sum_{k=1}^L a_{kq} [\cos(\phi_{km}) \cos(\theta_{kq}) - \sin(\phi_{km}) \sin(\theta_{kq})] = 0 \quad m=1,2,\dots,N; m \neq q \quad (2.21)$$

Equation 2.17 (imaginary terms with source present at the "q th" depth) becomes

$$\sum_{k=1}^L -a_{kq} (\sin(\phi_{kq}) \cos(\theta_{kq}) + \cos(\phi_{kq}) \sin(\theta_{kq})) = 0 \quad (2.22)$$

and equation 2.19 (imaginary terms with source absent for each of the other 'N-1' depths) becomes

$$\sum_{k=1}^L -a_{kq} [\sin(\phi_{km}) \cos(\theta_{kq}) + \cos(\phi_{km}) \sin(\theta_{kq})] = 0 \quad m=1,2,\dots,N; m \neq q \quad (2.23)$$

Thus, there are a total of '2N' equations with '2L' unknowns.

In order to simplify, we put these '2N' equations into matrix form. Arbitrarily the real terms are made the first 'N' equations and the imaginary terms the second 'N' equations. The first real and first imaginary equation is at the lowest (shallowest) source depth and equations increase in order after that until the last real and last imaginary equation correspond to a source at the deepest depth. The resultant matrix equation becomes:

$$\begin{bmatrix} 0 \\ 0 \\ \vdots \\ 0 \\ L \\ 0 \\ \vdots \\ 0 \\ 0 \\ \vdots \\ 0 \end{bmatrix} = \begin{bmatrix} \cos\phi_{11} & \cos\phi_{21} & \dots & \cos\phi_{L1} & -\sin\phi_{11} & -\sin\phi_{21} & \dots & -\sin\phi_{L1} \\ \cos\phi_{12} & \cos\phi_{22} & \dots & \cos\phi_{L2} & -\sin\phi_{12} & -\sin\phi_{22} & \dots & -\sin\phi_{L2} \\ \vdots & \vdots & & \vdots & \vdots & \vdots & & \vdots \\ \cos\phi_{1q} & \cos\phi_{2q} & \dots & \cos\phi_{Lq} & -\sin\phi_{1q} & -\sin\phi_{2q} & \dots & -\sin\phi_{Lq} \\ \vdots & \vdots & & \vdots & \vdots & \vdots & & \vdots \\ \cos\phi_{1N} & \cos\phi_{2N} & \dots & \cos\phi_{LN} & -\sin\phi_{1N} & -\sin\phi_{2N} & \dots & -\sin\phi_{LN} \\ -\sin\phi_{11} & -\sin\phi_{21} & \dots & -\sin\phi_{L1} & -\cos\phi_{11} & -\cos\phi_{21} & \dots & -\cos\phi_{L1} \\ -\sin\phi_{12} & -\sin\phi_{22} & \dots & -\sin\phi_{L2} & -\cos\phi_{12} & -\cos\phi_{22} & \dots & -\cos\phi_{L2} \\ \vdots & \vdots & & \vdots & \vdots & \vdots & & \vdots \\ -\sin\phi_{1N} & -\sin\phi_{2N} & \dots & -\sin\phi_{LN} & -\cos\phi_{1N} & -\cos\phi_{2N} & \dots & -\cos\phi_{LN} \end{bmatrix} \begin{bmatrix} a_{1q} \cos\theta_{1q} \\ a_{2q} \cos\theta_{2q} \\ \vdots \\ a_{Lq} \cos\theta_{Lq} \\ a_{1q} \sin\theta_{1q} \\ a_{2q} \sin\theta_{2q} \\ \vdots \\ a_{Lq} \sin\theta_{Lq} \end{bmatrix} \quad (2.24)$$

Simplifying further, equation 2.24 becomes:

$$\begin{bmatrix} 0 \\ \vdots \\ L \\ \vdots \\ 0 \\ \hline 0 \end{bmatrix} = \begin{bmatrix} \underline{\alpha} & -\underline{\beta} \\ \hline -\underline{\beta} & -\underline{\alpha} \end{bmatrix} \begin{bmatrix} \underline{c} \\ \hline \underline{s} \end{bmatrix} \quad (2.25)$$

where ' α ', ' β ', ' c ', and ' s ' represent the appropriate submatrices.

Then, by noting that the multiplication of each element of a column by the same nonzero constant doesn't affect the solution, equation 2.25 becomes:

$$\begin{bmatrix} 0 \\ \vdots \\ L \\ \vdots \\ 0 \\ \hline 0 \end{bmatrix} = \begin{bmatrix} \underline{\alpha} & \underline{\beta} \\ \hline -\underline{\beta} & \underline{\alpha} \end{bmatrix} \begin{bmatrix} \underline{c} \\ \hline \underline{s} \end{bmatrix} \quad (2.26)$$

Finally letting Z , A , and Θ represent the matrices in equation 2.26, we obtain

$$\underline{Z} = \underline{A}\underline{\Theta} \quad (2.27)$$

where a matrix is denoted by a capitalized underlined letter.

In summary, Z is the desired response of the vertical array to the ' N ' source test depths. A represents known travel times from each of the ' N ' source depths to each of the ' L ' receiving hydrophones. Θ is unknown. It is the phase and amplitude weighting which must be applied to the vertical array in order to realize Z . Θ contains ' $2L$ ' unknowns.

Equation 2.27 represents '2N' equations. Since this system of equations is overdetermined ($N > L$) an exact solution does not exist. In order to make the best estimate of $\underline{\theta}$ for the desired response, the linear minimum variance estimation technique is used.

C. LINEAR MINIMUM VARIANCE METHOD

Equation 2.27 represents a noise free environment. If noise were present it would become

$$\underline{Z} = \underline{A}\underline{\theta} + \underline{n} \quad (2.28)$$

with ' \underline{n} ' a "2N" element column vector. This represents the noise at each source depth. ' \underline{Z} ' is a linear function of ' $\underline{\theta}$ ' and is called the observation. ' \underline{A} ' is a "2Nx2L" modulation or observation matrix which is known, and ' $\underline{\theta}$ ' is the "2L" element random parameter vector which is to be estimated. Assume the first and second moments of ' $\underline{\theta}$ ' and ' \underline{n} ' are given by

$$E(\underline{\theta}) = \underline{\mu}_{\theta} \quad \text{Var}(\underline{\theta}) = \underline{V}_{\theta} \quad (2.29)$$

and

$$E(\underline{n}) = \underline{0} \quad \text{Var}(\underline{n}) = \underline{V}_n \quad (2.30)$$

where 'E' represents expectation or first moment and 'Var' represents the covariance matrix. It is assumed that the parameter ' $\underline{\theta}$ ' and the noise ' \underline{n} ' are uncorrelated.

A restriction imposed is that the estimate must be a weighted linear combination of the observations:

$$\hat{\underline{\theta}}_L = \underline{b} + \underline{E}\underline{Z} \quad (2.31)$$

where '^' indicates estimate. The objective is to select 'b' and 'B' in order to minimize the error variance. Such an estimator is the linear minimum variance estimator; it is the best, in the sense of minimum-error-variance linear estimators.

Another restriction is that the estimator be unbiased; in other words it is required that the expected value of the estimator ' $\hat{\underline{\theta}}_L$ ' is equal to the expected value of the parameter 'θ'. Thus,

$$E(\hat{\underline{\theta}}_L) = \underline{b} + \underline{E}E(\underline{Z}) = E(\underline{\theta}) = \underline{\mu}_\theta \quad (2.32)$$

yielding

$$\underline{b} = \underline{\mu}_\theta - \underline{E}\underline{A}\underline{\mu}_\theta \quad (2.33)$$

Substituting this result in equation 2.31 gives for the unbiased linear estimator

$$\hat{\underline{\theta}}_L = \underline{\mu}_\theta + \underline{E}(\underline{Z} - \underline{A}\underline{\mu}_\theta) \quad (2.34)$$

Note that since the estimator is unbiased, the estimation error ' $\underline{\theta}_E = \underline{\theta} - \hat{\underline{\theta}}_L$ ' is zero mean. The next step is to select 'B' in order to minimize the error variance. However, this optimization problem is ill-defined because the error variance is a matrix. Therefore in order to introduce a scalar goodness measure the sum of the variances of each component of 'θ' is minimized. This is the sum of the main diagonal terms of the covariance matrix and is defined as the trace of the matrix.

$$\text{tr} (\text{Var}(\underline{\theta}_E)) = \sum_{n=1}^{2N} \text{Var}((\underline{\theta}_E)_n) \quad (2.35)$$

where 'tr' indicates trace. 'B' is then selected to minimize the trace of the error variance, or

$$\min_B \text{tr} (\text{Var}(\underline{\theta}_E)) = \min_B \text{tr} (E(\underline{\theta}_E \underline{\theta}_E^T)) \quad (2.36)$$

where '^T' indicates the transpose. The following problem is then obtained by substituting equation 2.34 into equation 2.36:

$$\min_B \text{tr} (\text{Var}(\underline{\theta}_E)) = \min_B \text{tr} (E((\underline{\theta} - \underline{u}_\theta - \underline{B}(\underline{Z} - \underline{A}\underline{u}_\theta))(\underline{\theta} - \underline{u}_\theta - \underline{B}(\underline{Z} - \underline{A}\underline{u}_\theta))^T)) \quad (2.37)$$

It is well known [Ref. 3] that equation 2.37 is minimized when

$$\text{Cov}(\underline{\theta}, \underline{Z}) - \underline{B} \text{Var}(\underline{Z}) = \underline{0} \quad (2.38)$$

where 'Cov(θ, Z)' is the covariance matrix of the unknown parameters and the observations. Denoting the optimum filter by 'B^{*}', then if

$$\underline{B}^* = \text{Cov}(\underline{\theta}, \underline{Z}) (\text{Var}(\underline{Z}))^{-1} \quad (2.39)$$

a minimum is achieved for the sum of the squares of the errors.

Using equation 2.28 for 'Z', the covariance of 'θ' and 'Z' becomes

$$\text{Cov}(\underline{\theta}, \underline{Z}) = \text{Cov}(\underline{\theta}, \underline{A}\underline{\theta} + \underline{n}) = \underline{V}_\theta \underline{A}^T \quad (2.40)$$

since 'θ' and 'n' are uncorrelated. The variance of 'Z' is

$$\text{Var}(\underline{Z}) = \text{Var}(\underline{A}\underline{\theta} + \underline{n}) = \underline{A}\underline{V}_{\underline{\theta}}\underline{A}^T + \underline{V}_{\underline{n}} \quad (2.41)$$

Substituting these into equation 2.39 gives

$$\underline{B}^* = \underline{V}_{\underline{\theta}}\underline{A}^T(\underline{A}\underline{V}_{\underline{\theta}}\underline{A}^T + \underline{V}_{\underline{n}})^{-1} \quad (2.42)$$

and the linear minimum variance estimator is

$$\hat{\underline{\theta}}_{\text{LMV}} = \underline{\mu}_{\underline{\theta}} + \underline{V}_{\underline{\theta}}\underline{A}^T(\underline{A}\underline{V}_{\underline{\theta}}\underline{A}^T + \underline{V}_{\underline{n}})^{-1}(\underline{Z} - \underline{A}\underline{\mu}_{\underline{\theta}}) \quad (2.43)$$

By utilizing a matrix inversion lemma [Ref. 3] equation 2.43 becomes

$$\hat{\underline{\theta}}_{\text{LMV}} = (\underline{A}^T\underline{V}_{\underline{n}}^{-1}\underline{A} + \underline{V}_{\underline{\theta}}^{-1})^{-1}(\underline{A}^T\underline{V}_{\underline{n}}^{-1}\underline{Z} + \underline{V}_{\underline{\theta}}^{-1}\underline{\mu}_{\underline{\theta}}) \quad (2.44)$$

The advantage of this equation over equation 2.43 is the size of the matrix to be inverted. In equation 2.43 the matrix has dimensionality '2N' while in equation 2.44 its dimensionality is only '2L'. Thus the advantages of the linear variance estimator are the ease with which they are derived, the mathematical tractability of the linear form, and the minimum amount of stochastic information required for development. An interesting characteristic is that the linear minimum variance estimate is the orthogonal projection of ' θ ' onto the space spanned by the observation ' Z '. Because of these factors this estimator is a popular form for estimating unknowns in overdetermined equations.

For this thesis it is assumed that the noise samples are uncorrelated and identically distributed so that:

$$\underline{V}_{\underline{n}} = \sigma^2 \underline{I} \quad (2.45)$$

No previous knowledge is assumed about ' θ '. This implies an infinite variance matrix which is represented as:

$$\underline{v}_{\theta}^{-1} = \underline{0} \quad \text{and} \quad \underline{\mu}_{\theta} = \underline{0} \quad (2.46)$$

The linear minimum variance estimate given by equation 2.44 is then

$$\hat{\underline{\theta}}_{\text{LMV}} = (\underline{A}^T \underline{A})^{-1} \underline{A}^T \underline{Z} \quad (2.47)$$

By determining ' $\hat{\underline{\theta}}_{\text{LMV}}$ ', the phase and amplitude weights are found for a signal source on the ' q th' depth. Recall that

$$\hat{\underline{\theta}}_{\text{LMV}} = \begin{bmatrix} \hat{\theta}_1 \\ \hat{\theta}_2 \\ \vdots \\ \hat{\theta}_L \\ \hat{\theta}_{L+1} \\ \vdots \\ \hat{\theta}_{2L} \end{bmatrix} = \begin{bmatrix} a_{1q} \cos \theta_{1q} \\ a_{2q} \cos \theta_{2q} \\ \vdots \\ a_{Lq} \cos \theta_{Lq} \\ a_{1q} \sin \theta_{1q} \\ \vdots \\ a_{Lq} \sin \theta_{Lq} \end{bmatrix} \quad (2.48)$$

Upon solving, this equation gives for the phase delay

$$\hat{\theta}_{mq} = \arctan(\hat{\theta}_{L+m} / \hat{\theta}_m) \quad \text{where } m=1 \text{ to } L \quad (2.49)$$

and amplitude weight

$$\hat{a}_{mq} = \hat{\theta}_m / \cos(\hat{\theta}_{mq}) \quad \text{where } m=1 \text{ to } L \quad (2.50)$$

When these amplitude weights and phase delays are applied to the vertical linear array a resulting beam pattern is formed which in the absence of noise is:

$$\hat{\underline{Z}} = \underline{A} \hat{\underline{\theta}}$$

(2.51)

The resulting beam pattern ' $\hat{\underline{Z}}$ ' can then be compared with the desired beam pattern ' \underline{Z} ', as well as with a conventional beam pattern ' \underline{Z} ' obtained using linear phase shifts across the array aperture selected to "steer" the array to the dominant arrival angle for the selected source depth.

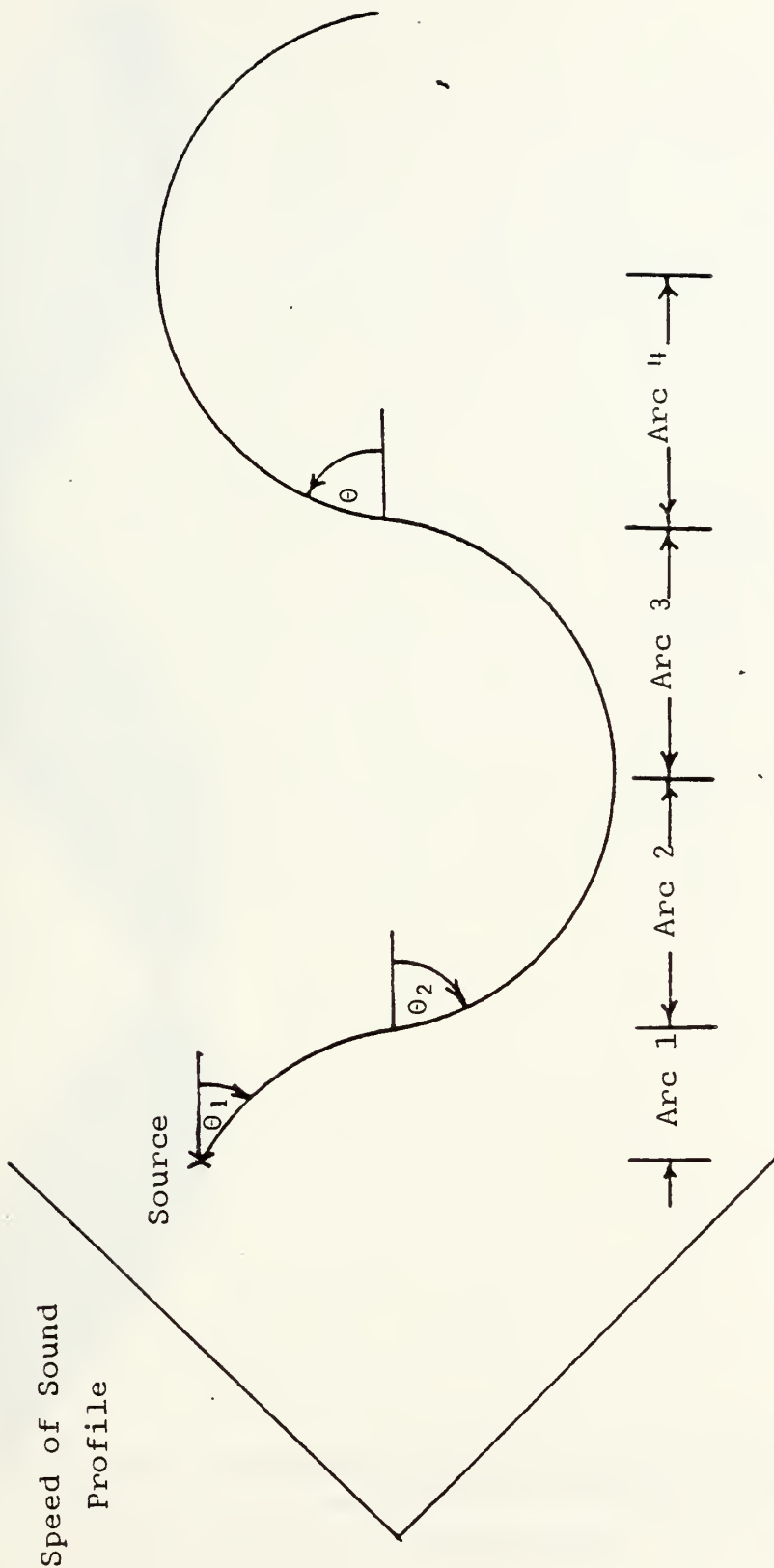


Figure 2.2 Single Ray Path Plot In Triangular SOFAR Channel

Vertical Linear Array

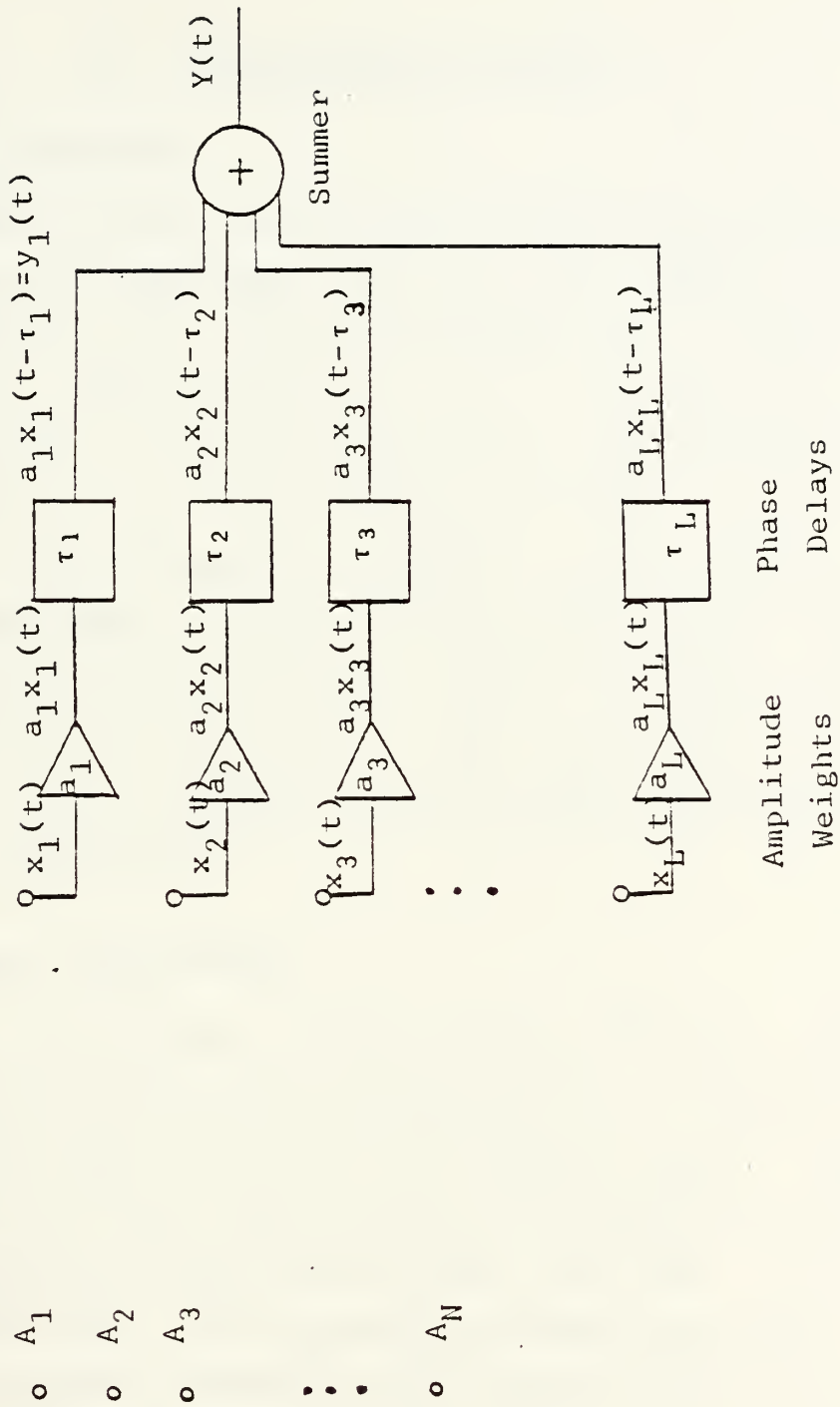


Figure 2.4 Array Model

III. EXPERIMENTAL PROCEDURE

A. BASIC ASSUMPTIONS

The speed of sound profile given in the Introduction was used to test the technique, with 'L', the number of source depths chosen as 20. The source depths are at 220 meters and every 20 meters thereafter to 600 meters inclusive. 'N', the number of hydrophones used in the vertical array was chosen as 5. The hydrophones are placed at depths of 100, 200, 300, 400, and 500 meters. Thus, there are 40 equations, two for each source depth, and 10 unknowns, two for each hydrophone. A range of 200 kilometers (km) assures that the deep sound channel is filled with sound over the aperture of the vertical linear array. A frequency of 100 Hz provides good resolution in the beam pattern without introducing alias mainlobes at the selected range across the depths of investigation.

B. 'A' MATRIX CALCULATION

Since the gradient of the sound velocity, 'g' is constant in the area of the source depths, and the speed of sound at the surface is known, equation 2.3 is used to solve for 'c2', the speed of sound at the source depth. Equation 2.7 is used for each source depth to calculate the maximum initial depression angle which yields R-R rays. In determining travel time, only depression angles from each source which are positive (downward) and yield R-R rays are used.

Beginning with the first source depth of 220 meters, an initial depression angle of 0.0 degrees is selected. The ray path is then calculated using equations 2.5 and 2.6 and broken into a series of arcs as in figure 2.2. Equation 2.9

is used to determine the travel time for each arc in the same manner. Each arc's horizontal range, travel time, and depth are summed. When the summed horizontal range reaches 200 km the summation process ends. The travel time and depth of the ray at this horizontal range is then known. The same procedure is repeated for an initial depression angle of 0.1 degrees and every increment of 0.1 degrees thereafter until the maximum depression from equation 2.7 is reached. The final ray path is at this maximum depression angle.

The same procedure is repeated for each of the other 19 source depths.

Thus, for each initial angle from each source depth there is a ray which has a travel time and a depth when it reaches the horizontal range of 200 km. Since it is the profile of the sound pressure wave which impinges on the vertical array which is of importance, a constant can be subtracted from these calculated travel times. This constant is selected to be the travel time for the source depth of 220 meters which has an initial depression angle of 0 degrees. It is subtracted from each of the travel times making the resultant travel times relative with respect to the ray which has a 0 degree depression angle from the 220 meter depth. The program and its listing which calculates the relative travel times and the depths of these rays at the horizontal range of 200 km is given in Appendix A.

A plot of the relative travel times versus depth for the 220 meter source depth is shown in Figure 3.1. Figure 3.2 displays the plot for the 380 meter source depth. Negative relative travel times in the plots indicate that the overall travel time is less than the reference. These rays arrive at the 200 km horizontal distance before the reference ray.

Since the receiving hydrophones are at set vertical positions (100, 200, 300, 400, and 500 meters), an

interpolation is done to determine relative travel times to them from each source depth. The interpolation program and its listing is in Appendix B. Sometimes more than one R-R ray travels from the source depth to a hydrophone. When this occurs, the ray which arrives first is used in the calculation of relative travel time to that hydrophone.

Equation 2.12 determines the phase shift relating to the relative travel times. The 'A' matrix is formed by taking the appropriate sine and cosine values as in equation 2.24. The 'A' matrix is '40 by 10'.

C. 'Z' MATRIX

Referring to equation 2.26, the 'Z' matrix is a '40 by 1' column vector. It is the desired beam pattern. The bottom 20 rows give the imaginary terms and are set to zero. The top 20 rows represent the value of the real terms at each source depth. Therefore each of the top 20 rows is set to zero except for the row containing the source. It is set to 1. For example, if the source is at 220 meters then only the top row is set to 1. If the source is at 380 meters then only the ninth row is set to 1.

D. RESULTING BEAM PATTERN

1. Using the Linear Minimum Variance Method

' \hat{e}_{LMV} ' is calculated using equation 2.47. The resulting beam pattern ' \hat{Z} ' is calculated using equation 2.51. The program which calculates the 'A' matrix, uses it in determining ' $\hat{\theta}_{LMV}$ ', and then calculates 'Z' is given in Appendix C. The program listing is also included.

2. Using Linear Phase Shifts

The conventional beam pattern is determined by using equation 2.51 where ' $\hat{\theta}$ ' is calculated by approximating the plot of relative travel time vs. depth by a straight line at the receiving hydrophone depths. For example Figure 3.3 represents this plot for the 380 meter source depth. The straight line is determined by a least squares linear regression which minimizes the sum of the squares of the deviations of the actual data points from the straight line of best fit. Note that only data points which are on the dominant curve are used in calculating the straight line. From the straight line, relative travel times to the receiving hydrophones are calculated. The relative travel times for the 380 meter source depth are given in Table I. They correspond to a plane wave arrival angle of 3.73 degrees. ' $\hat{\theta}$ ' is determined by converting these relative travel times to phase delays using equation 2.12 and then taking the appropriate sine and cosine values of these phase delays as in equation 2.24. The amplitude weights are initially assumed to be unity.

A second method for obtaining the conventional beam pattern is calculated by the same procedure except the amplitude weights which are determined by equation 2.50, the ' $\hat{\theta}_{LMV}$ ' amplitude weights, are applied to each hydrophone.

TABLE I

Relative Travel Times For 380 Meter Source Depth

<u>Hydrophone Depth</u>	<u>Relative Travel Time</u>
100 meters	-0.07565509 sec.
200 meters	-0.07131599 sec.
300 meters	-0.06697690 sec.
400 meters	-0.06263780 sec.
500 meters	-0.05829871 sec.

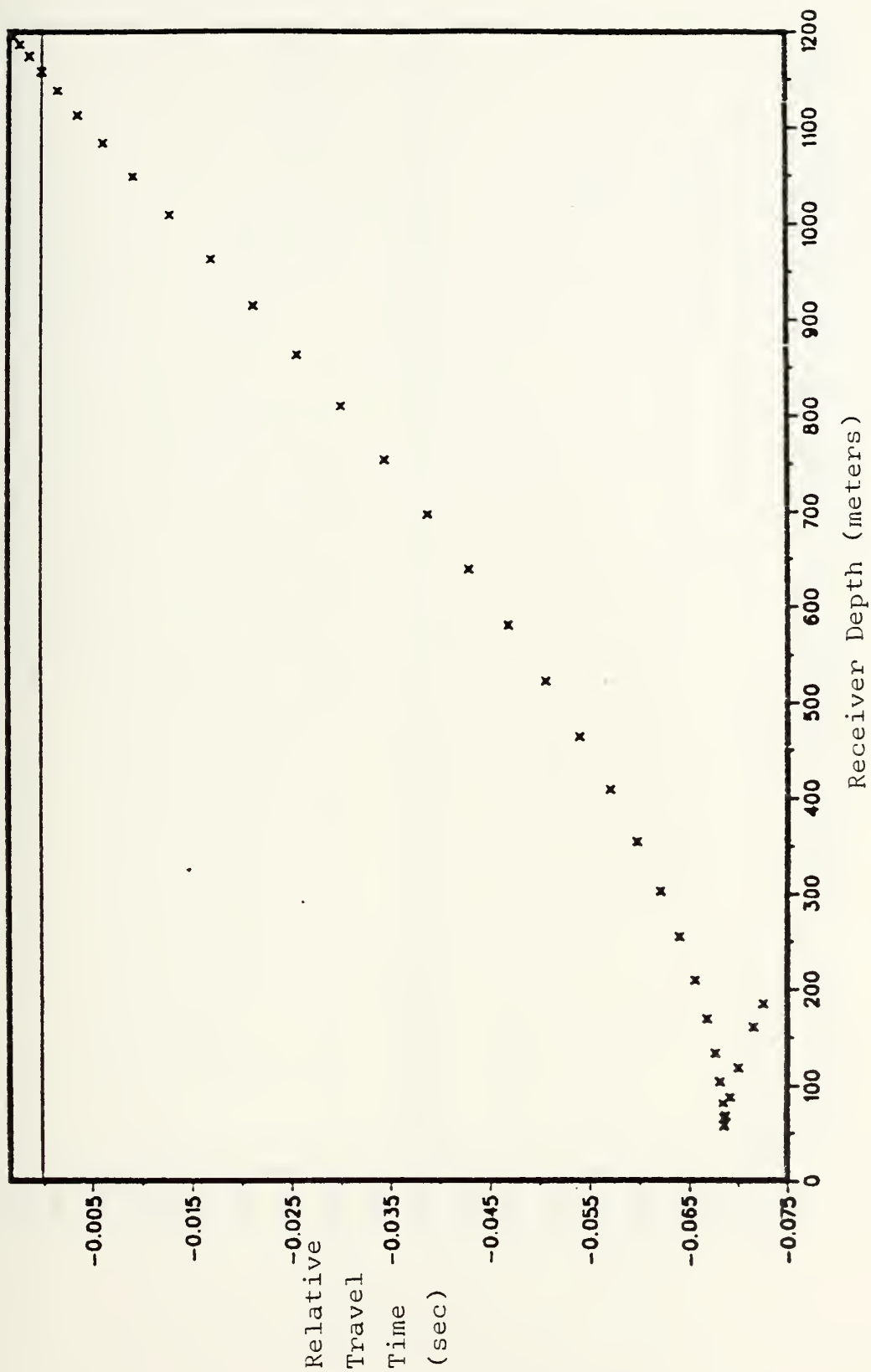


Figure 3.1 Relative Travel Time vs. Depth (220 meter source)

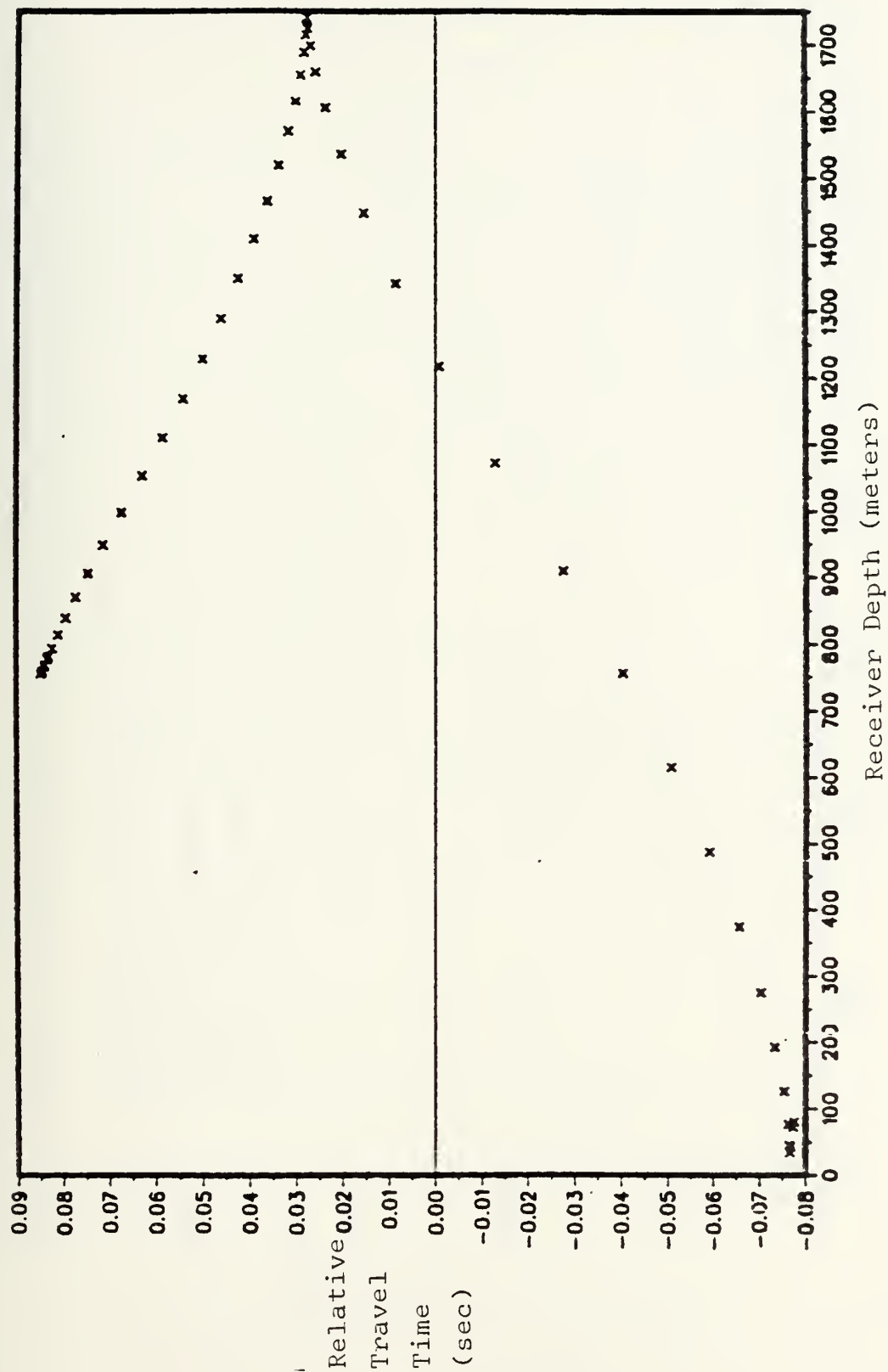


Figure 3.2 Relative Travel Time vs. Depth (380 meter source)

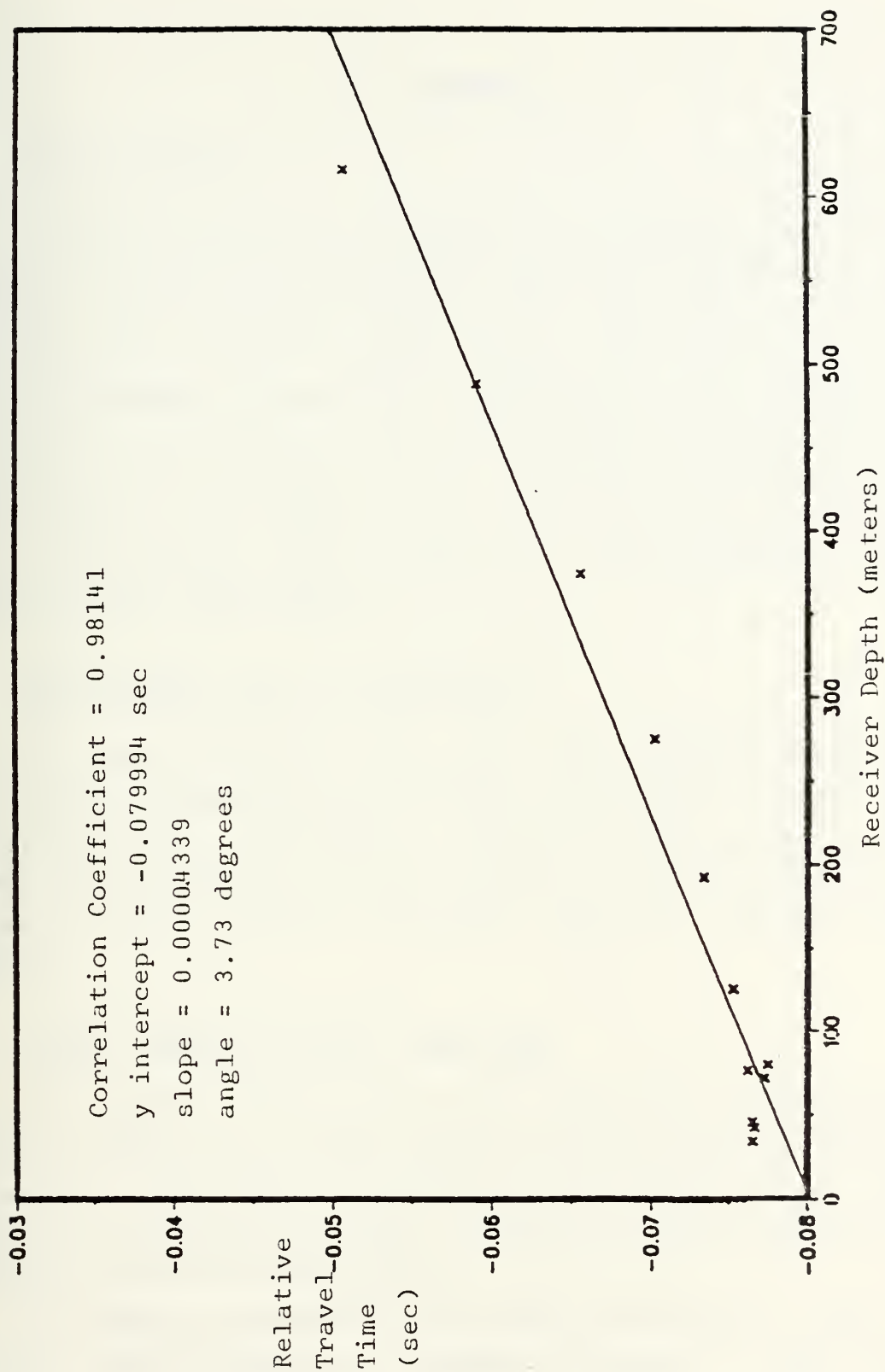


Figure 3.3 Straight Line Approx. of Rel. Trav. Time vs. Depth (source at 380 m)

IV. RESULTS

A. EXACT SOLUTION

An exact solution is derived for the beam pattern if the number of receiving hydrophones equal the number of source depths. For example, when the 5 receivers are used to discriminate between 5 source depths (220, 240, 260, 280, and 300 meters) there are 10 equations with 10 unknowns. Figure 4.1 is a plot of the resulting beam pattern with the source at the shallowest depth. Note that because of round-off errors in the 'IMSL' subroutines there is a small value for the resulting beam pattern at the non-energy source depths under investigation.

B. FOUR DEPTHS WITH TWO RECEIVERS

For source depths at 220, 280, 300, and 320 meters with receiving hydrophones at 100 and 200 meters, there are 8 equations with 4 unknowns. Figure 4.2 is a plot of the resulting beam pattern with a source at the 220 meter depth. Figure 4.3 is the plot for the source at the 280 meter depth.

C. TWENTY DEPTHS WITH TWO RECEIVERS

For all 20 source depths with receiving hydrophones at 100 and 200 meters, there are 40 equations with 4 unknowns. Figure 4.4 is a plot of the resulting beam pattern for a source at the 220 meter depth. Figure 4.5 is a plot for the source at the 380 meter depth.

In order to determine if the ' $\hat{\theta}$ ' calculated in this case is the best an alternate method is devised. Four source

depths (220, 240, 260 meters, and another source test depth) with the original source at the 220 meter depth and receivers at 100 and 200 meters are used. The beam pattern is calculated each time with a different source test depth substituted for the fourth source depth. The 5 best resulting beam patterns are selected along with the 8 source depths (220, 240, 260 meters, and the 5 test depths which created the 5 best beam patterns). Then, using these 8 source depths, ' $\hat{\theta}$ ' is determined for the two receivers. This ' $\hat{\theta}$ ' is applied to the two receivers and the beam pattern obtained for all 20 source depths.

The resulting beam pattern obtained by this alternate method isn't as good as the beam pattern obtained by using all 20 source depths in the determination of ' $\hat{\theta}$ '.

D. TWENTY DEPTHS WITH FIVE RECEIVERS

For all 20 source depths with all 5 receiving hydrophones there are 40 equations with 10 unknowns. Figure 4.6 is a plot of the resulting beam pattern with the source at the 220 meter depth. Figures 4.7, 4.8, and 4.9 are the plots for the source at the 360, 380, and 400 meter depths respectively.

E. CONVENTIONAL BEAMFORMER

Figure 4.10 is a plot of the beam pattern for a conventional beamformer using linear phase shifts across the array with the source at the 380 meter depth and the amplitude weights set to unity. All 20 source depths and 5 receiving hydrophones are used. Note that in figure 4.10 that there is less than 1 db discrimination between each of the source depths. Figure 4.11 is the plot obtained for the amplitude weights set to values determined by equation 2.50.

F. RANGE OF 250 KILOMETERS

The calculations were repeated for a range of 250 km using the same 20 source depths and 5 receiving hydrophones. Figures 4.12 and 4.13 represent the plots of relative travel times versus depth for the 220 and 380 meter source depths respectively. Figure 4.14 represents the straight line approximation of the relative travel times for the 380 meter depth. Note that in this figure the relative travel times are represented by two straight lines; the upper line represents linear phase shifts of the slower travel times for the conventional beamformer while the lower line represents linear phase shifts of the faster travel times. Tables II and III are the straight line interpolations of these slower and faster travel times which correspond to arrival angles of 4.04 and -3.16 degrees respectively. Figures 4.15 and 4.16 are the resulting beam patterns for the conventional beamformer for the slower travel times using unity amplitude weights and linear minimum variance amplitude weights respectively. Figures 4.17 and 4.18 are the beam patterns for the faster travel times.

Figures 4.19, 4.20, 4.21, and 4.22 represent plots of the beam pattern for the source at the 220, 340, 360, and 380 meter depths respectively.

TABLE II

Slower Ray Travel Times For 250 km Range and 380 m Source

<u>Hydrophone Depth</u>	<u>Relative Travel Time</u>
100 meters	-0.09949109 sec.
200 meters	-0.09478615 sec.
300 meters	-0.09008121 sec.
400 meters	-0.08537627 sec.
500 meters	-0.08067133 sec.

TABLE III

Faster Travel Times For 250 km Range and 380 m Source

<u>Hydrophone Depth</u>	<u>Relative Travel Time</u>
100 meters	-0.10100745 sec.
200 meters	-0.10468763 sec.
300 meters	-0.10836781 sec.
400 meters	-0.11204799 sec.
500 meters	-0.11572817 sec.

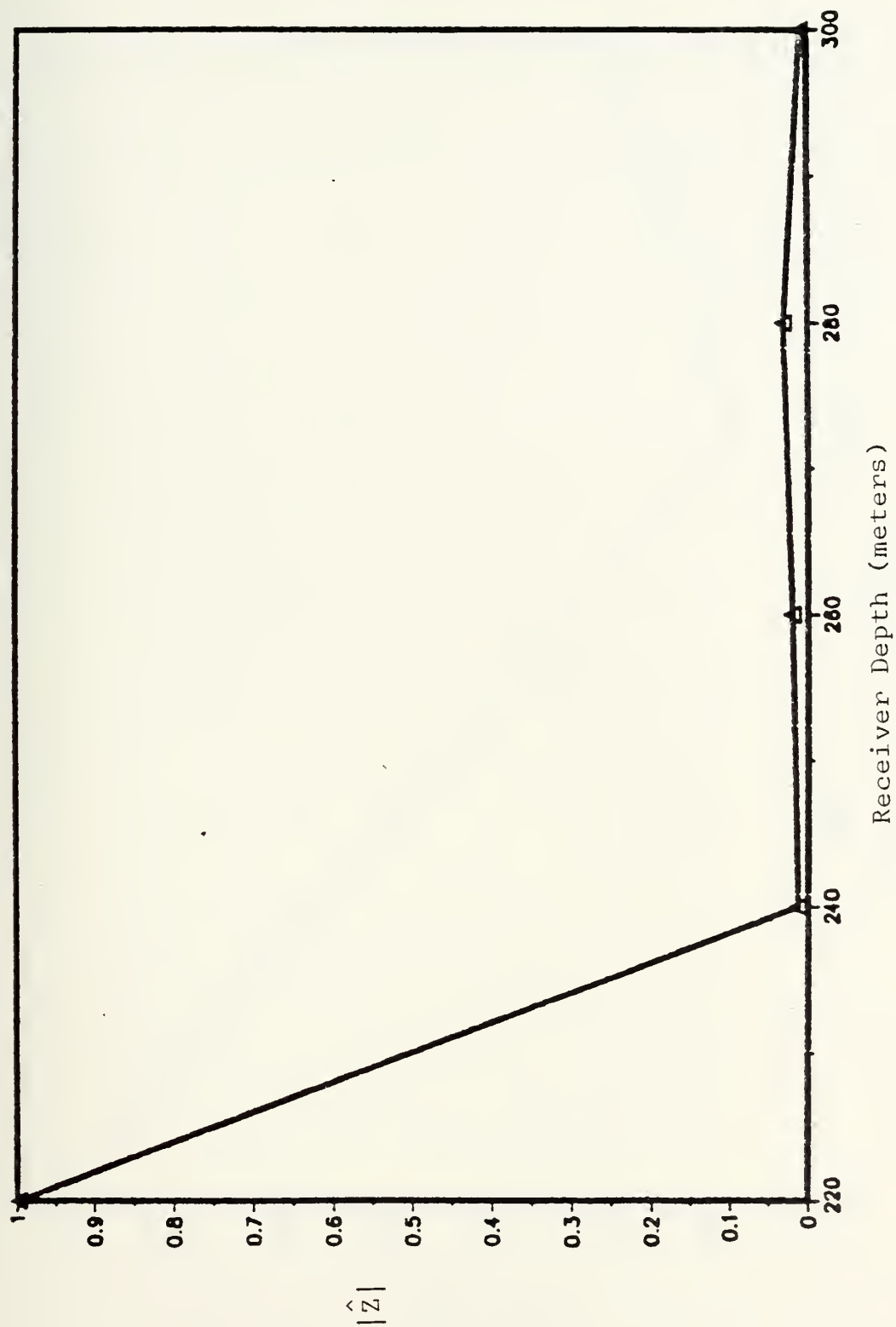


Figure 4.1 Beam Amplitude vs. Source Depth (5 depths 5 receivers)

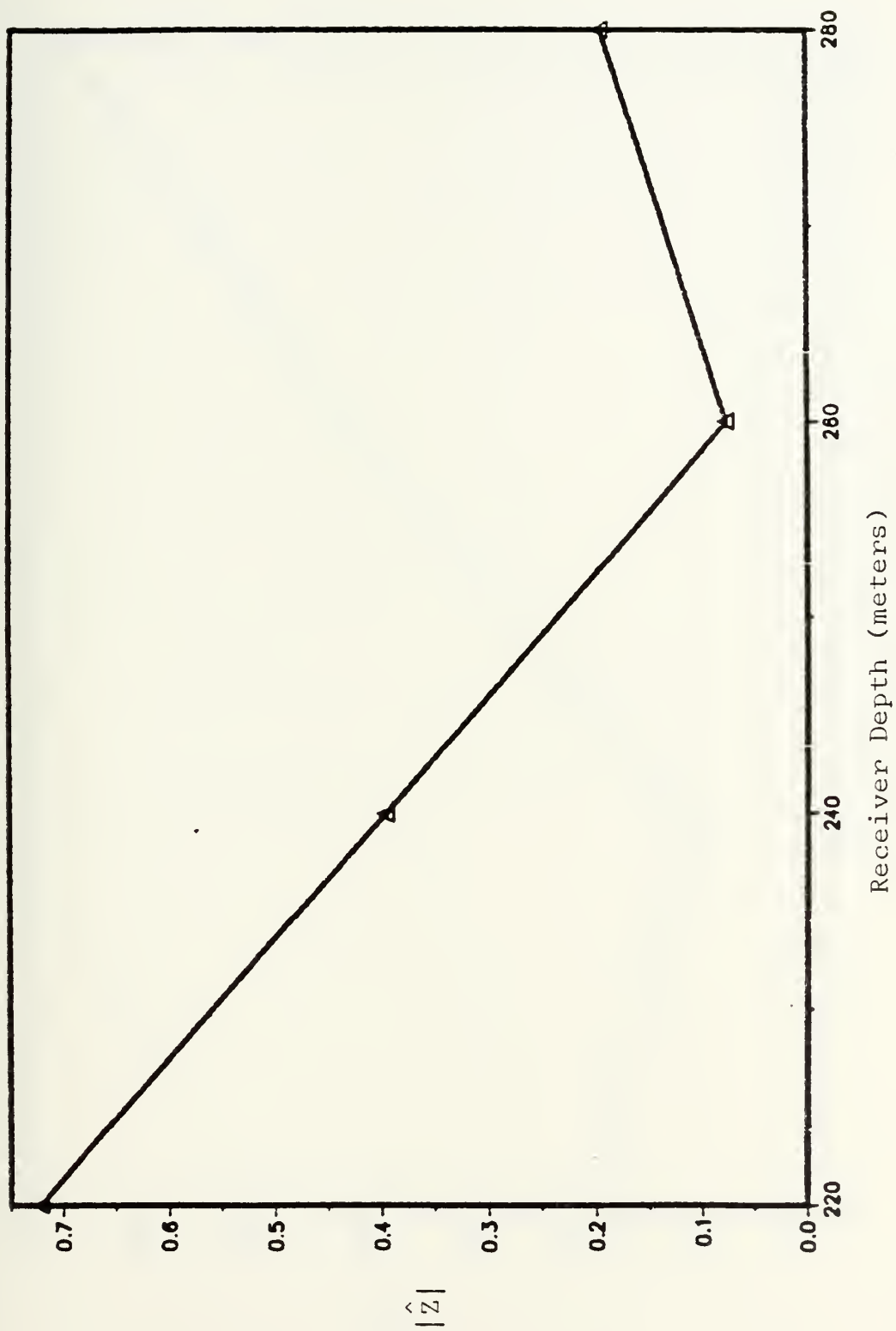


Figure 4.2 Beam Pattern (4 depths 2 receivers, source at 220 m)

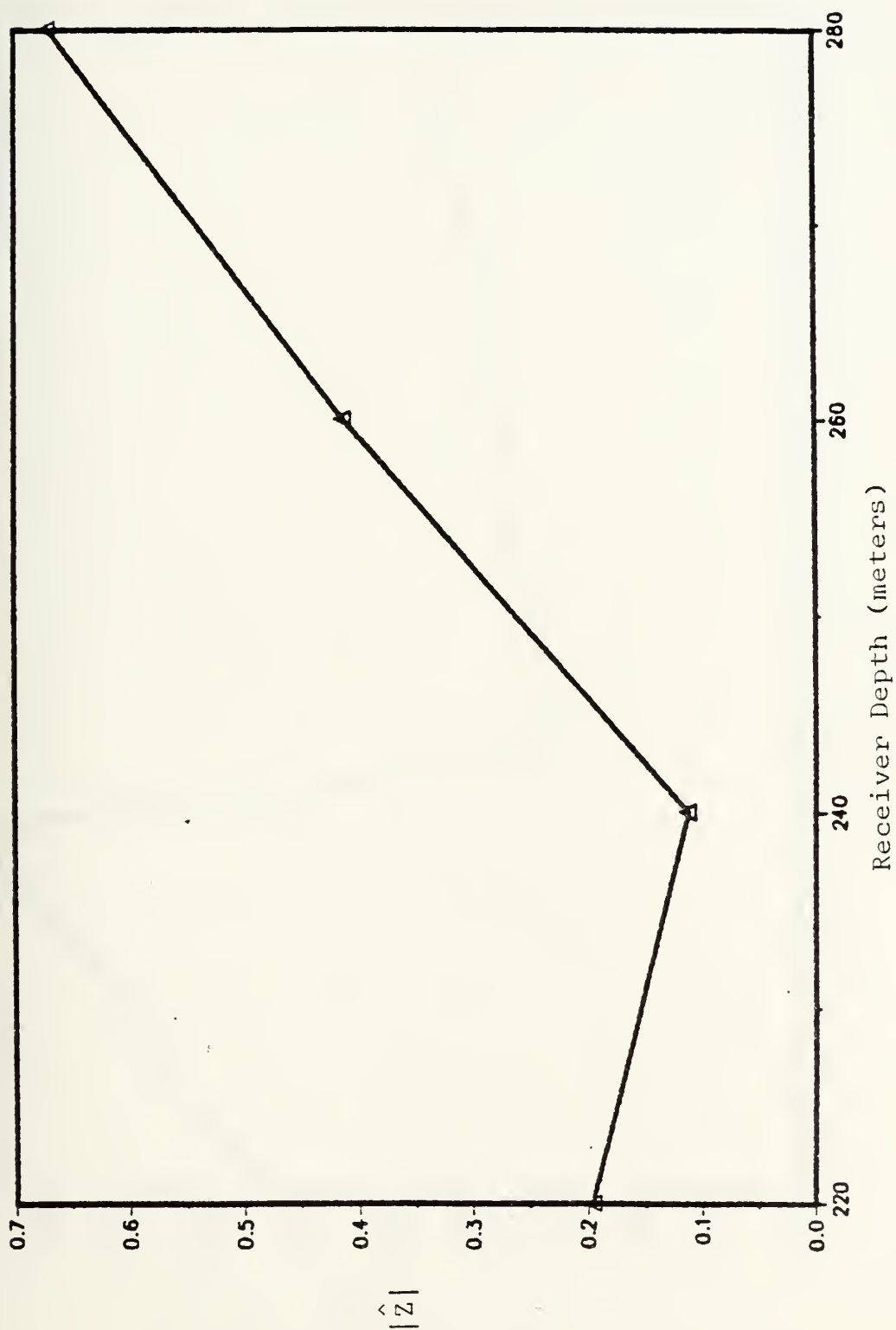


Figure 4.3 Beam Pattern (4 depths 2 receivers, source at 280 m)

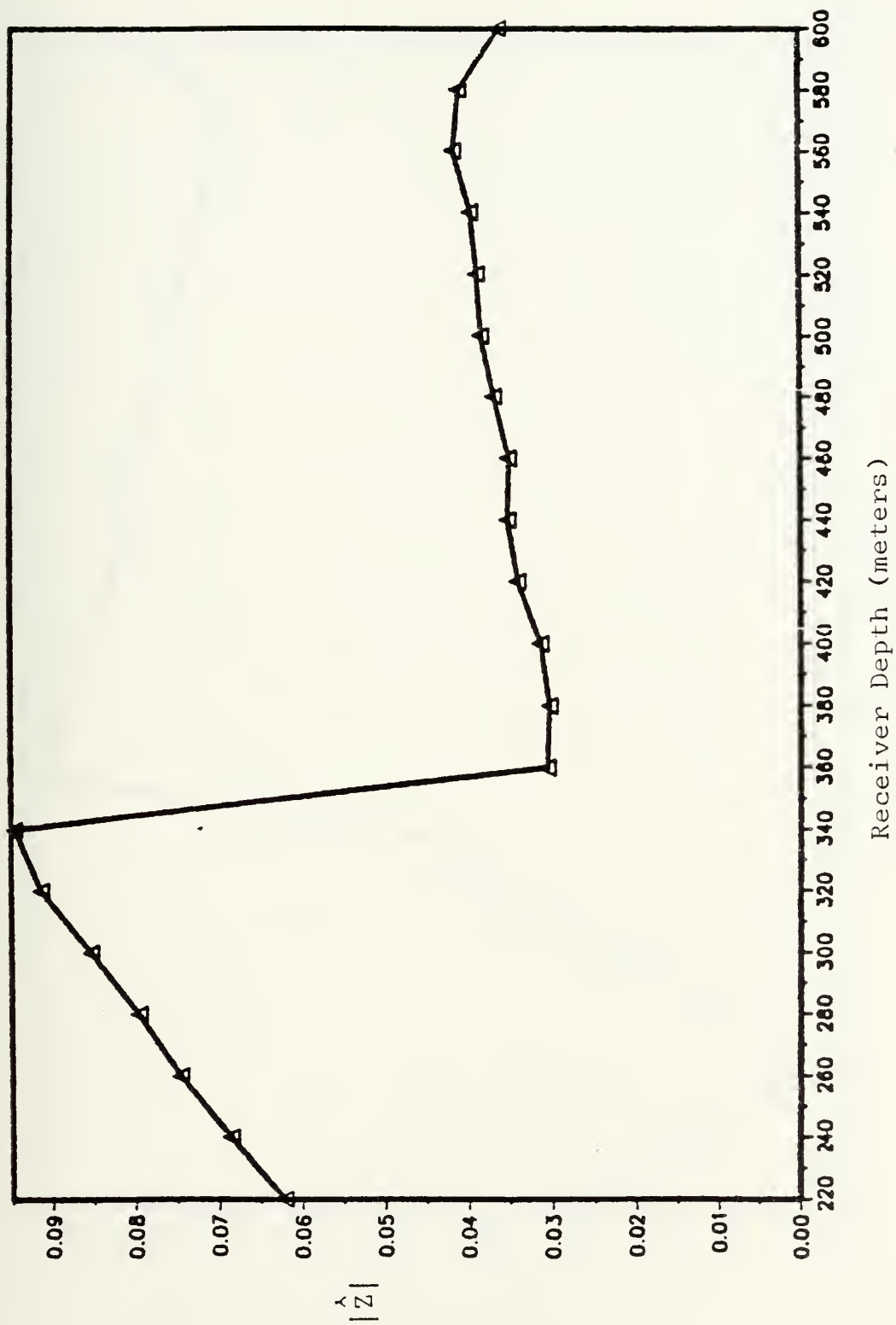


Figure 4.4 Beam Pattern (20 depths 2 receivers, source at 220 m)

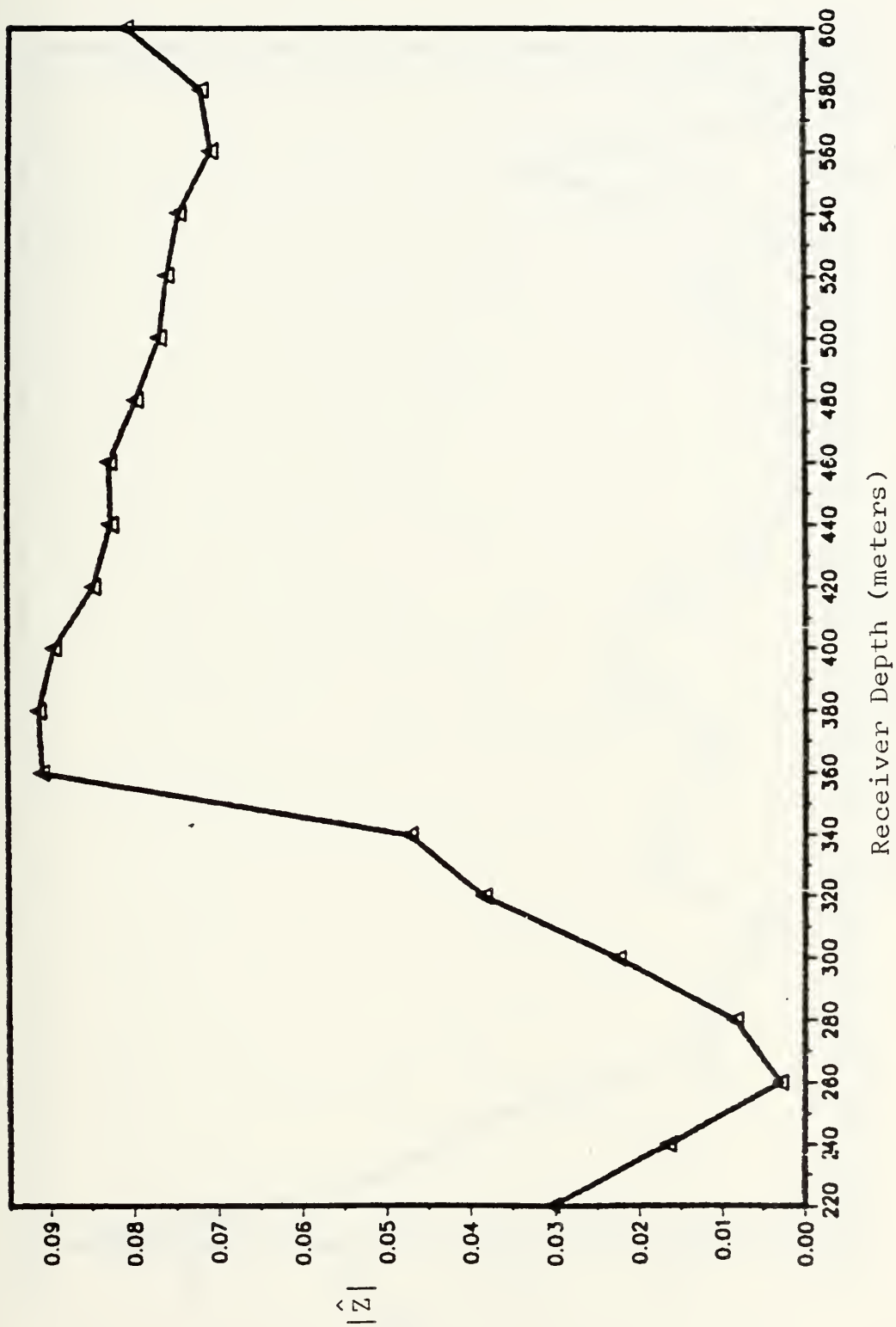


Figure 4.5 Beam Pattern (20 depths 2 receivers, source at 380 m)

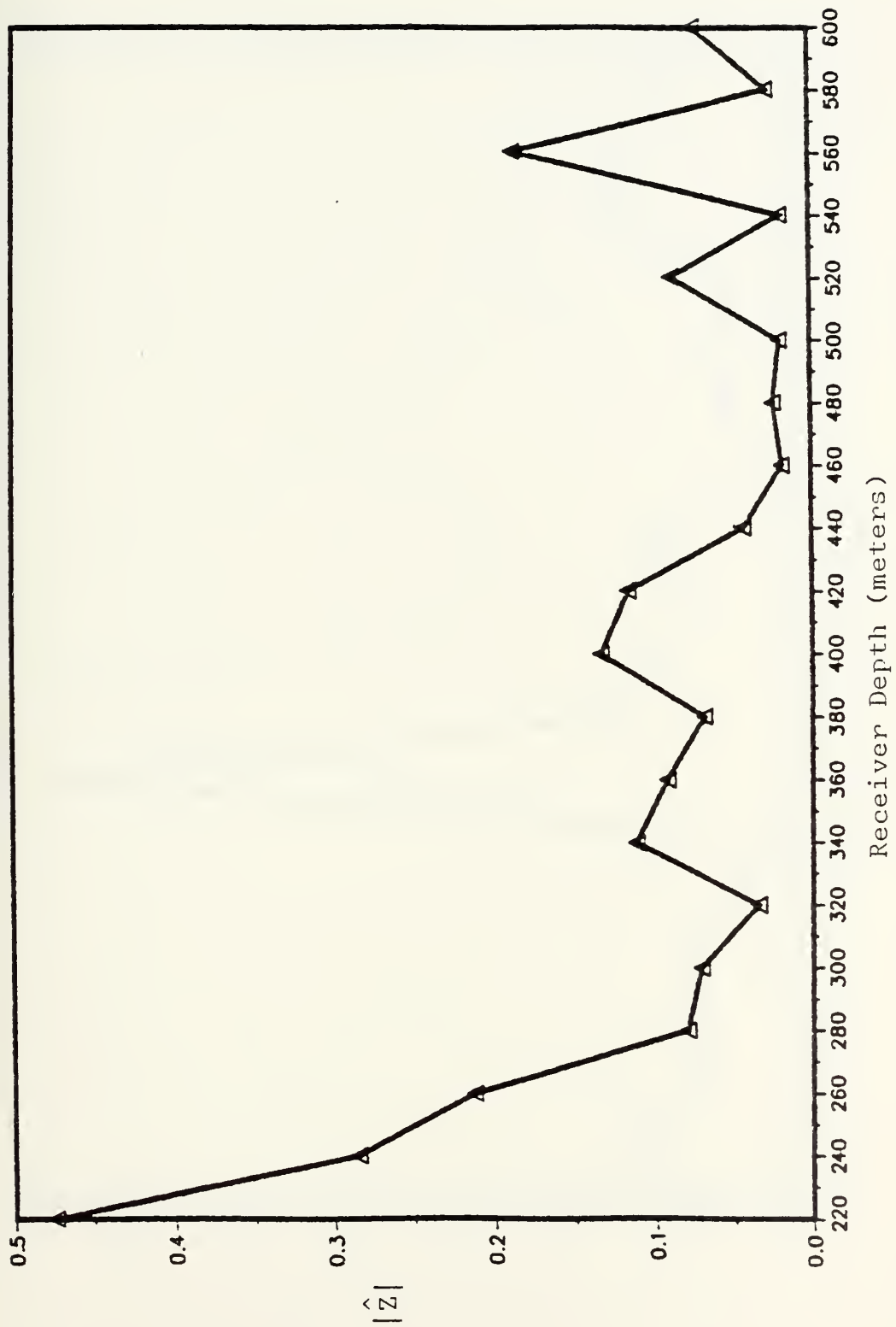


Figure 4.6 Beam Pattern (20 depths 5 receivers, source at 220 m)

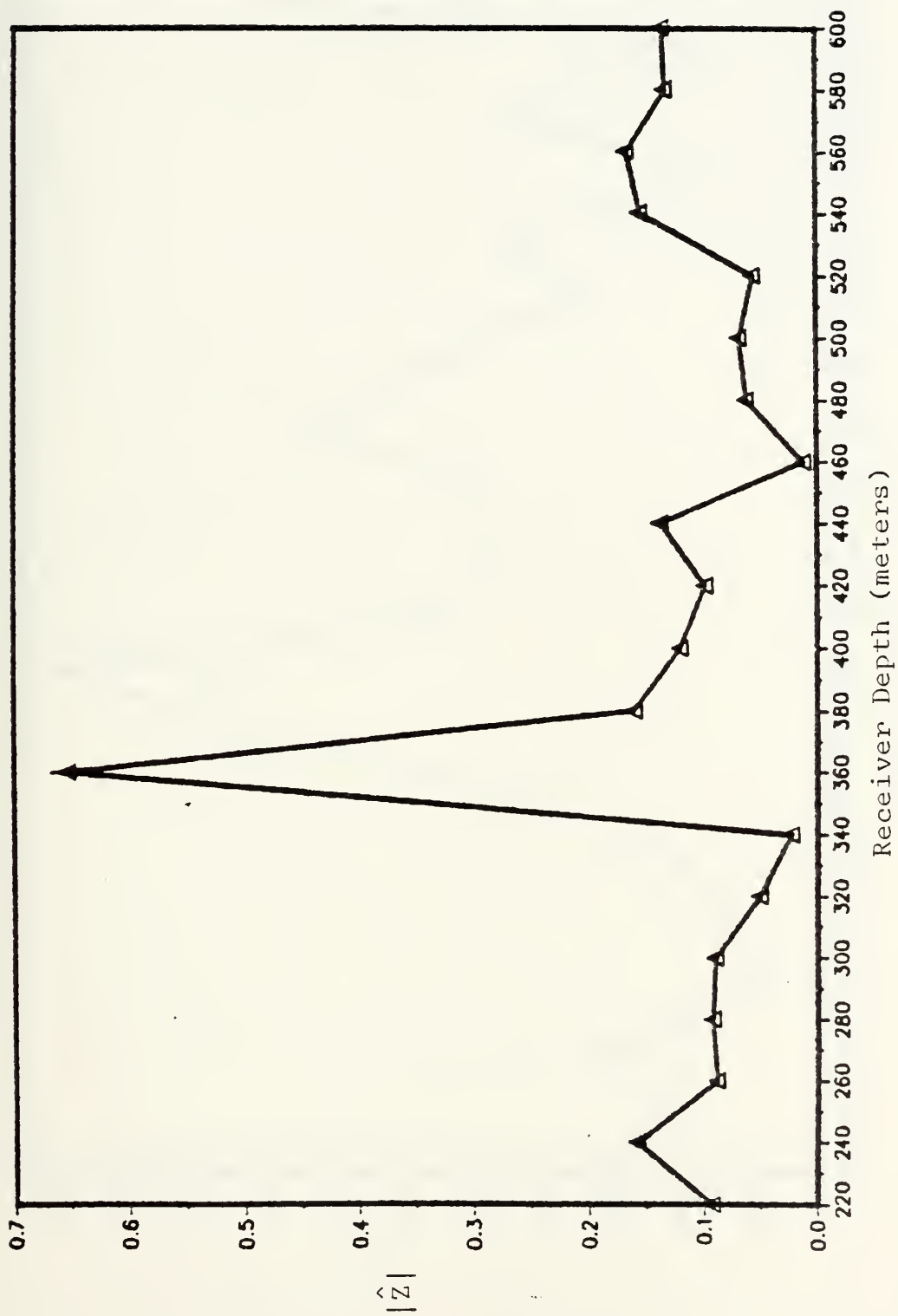


Figure 4.7 Beam Pattern (20 depths 5 receivers, source at 360 m)

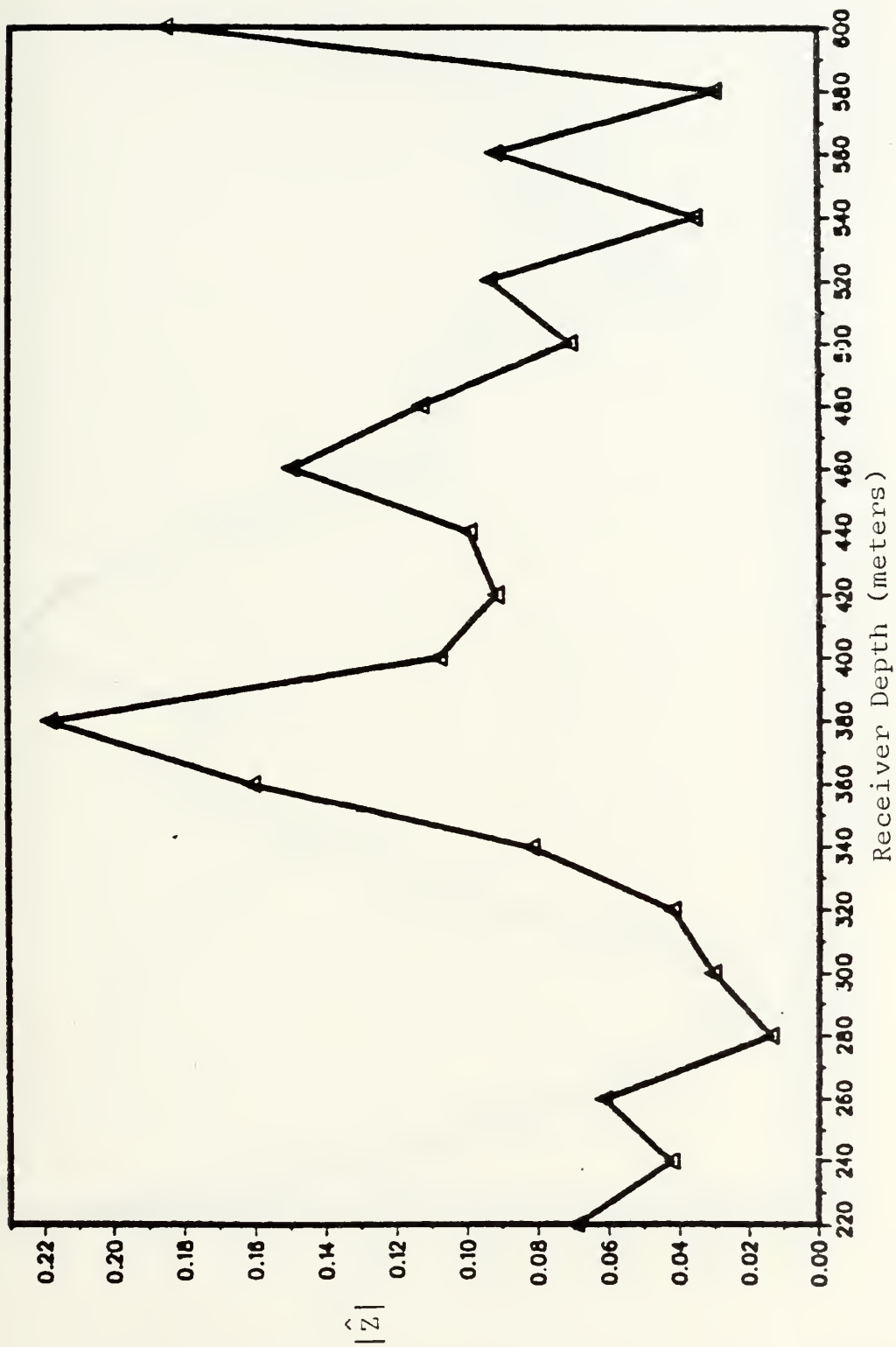


Figure 4.8 Beam Pattern (20 depths 5 receivers, source at 380 m)

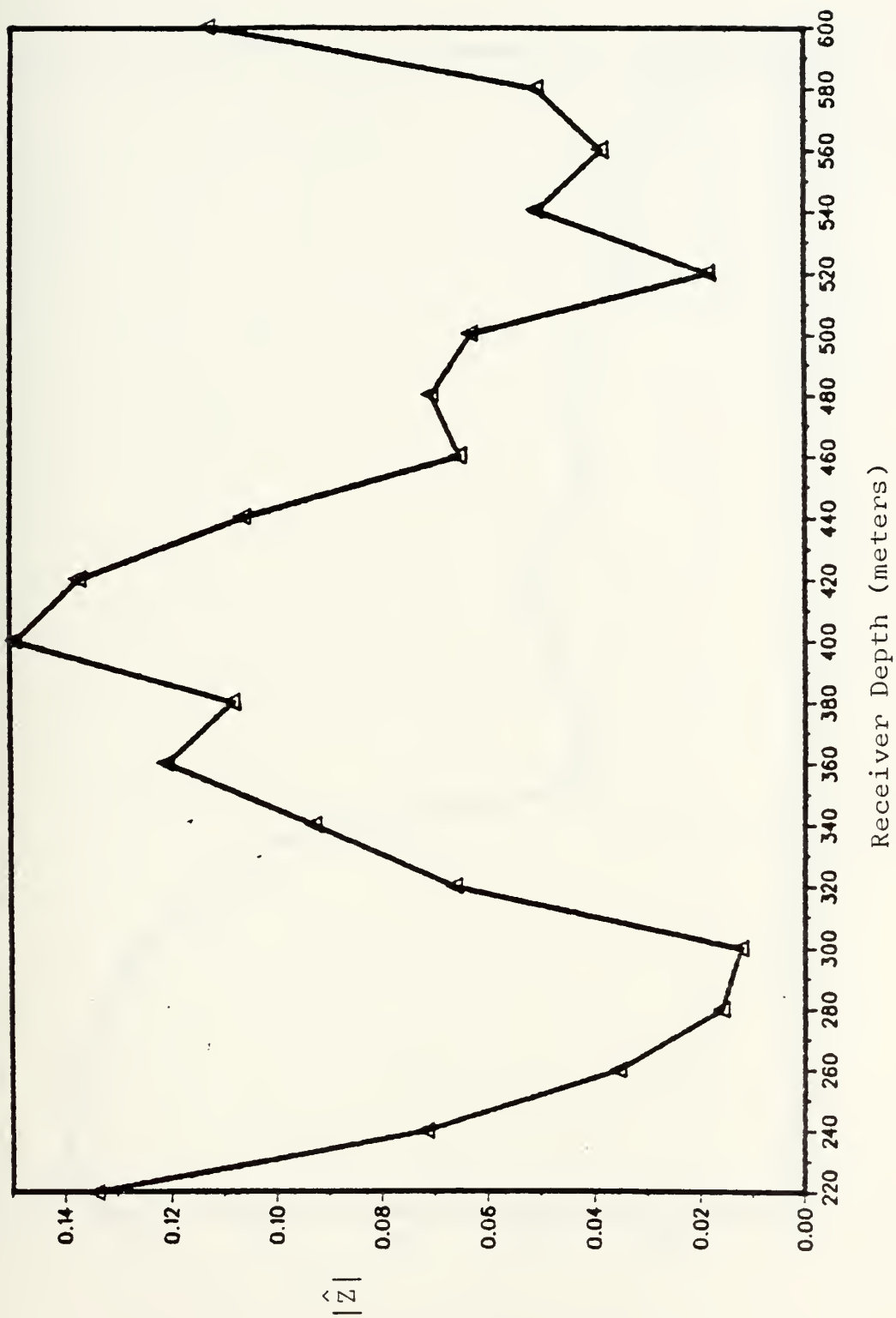


Figure 4.9 Beam Pattern (20 depths 5 receivers, source at 400 m)

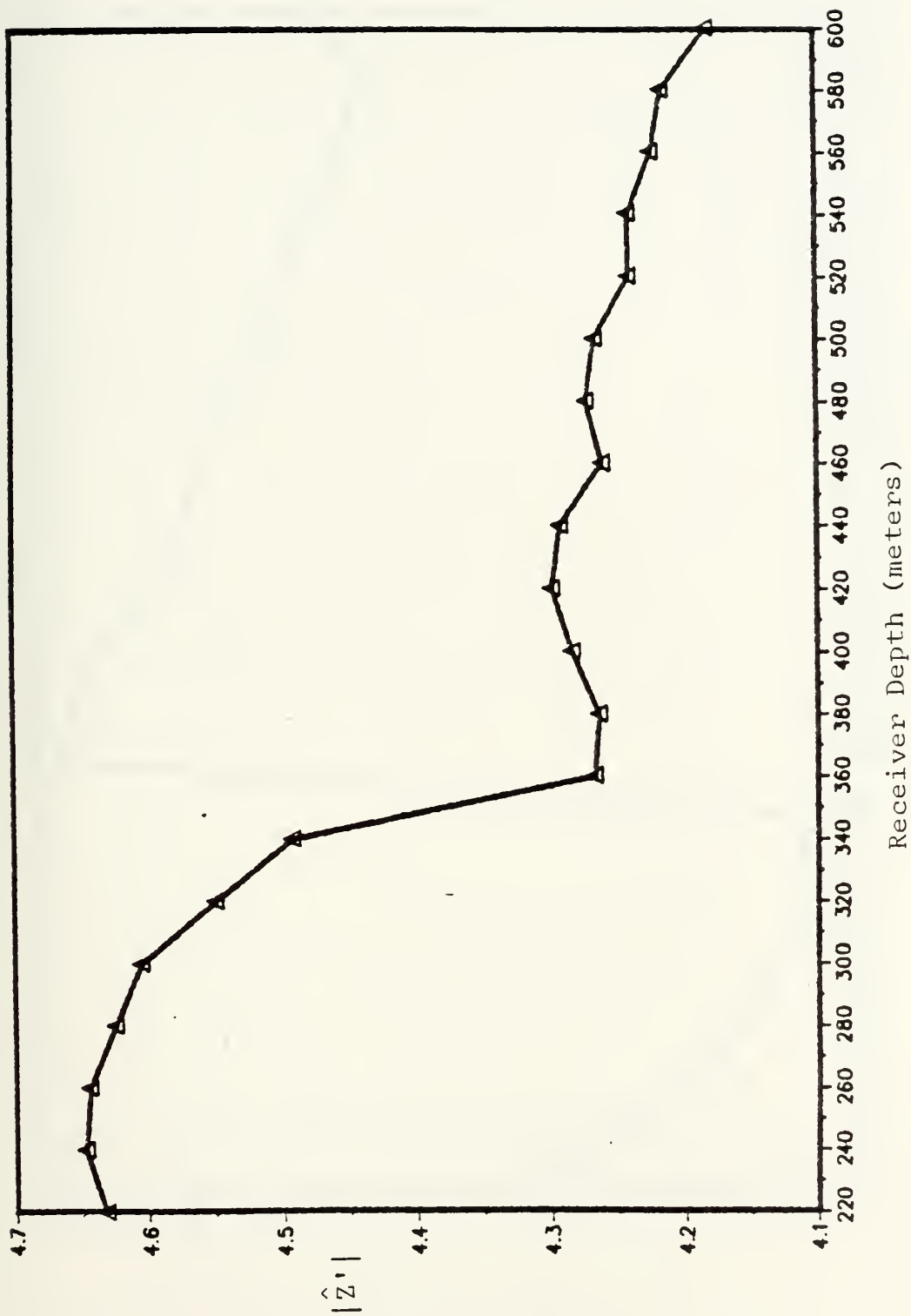


Figure 4.10 Conventional Beam Pattern (source at 380 meters)

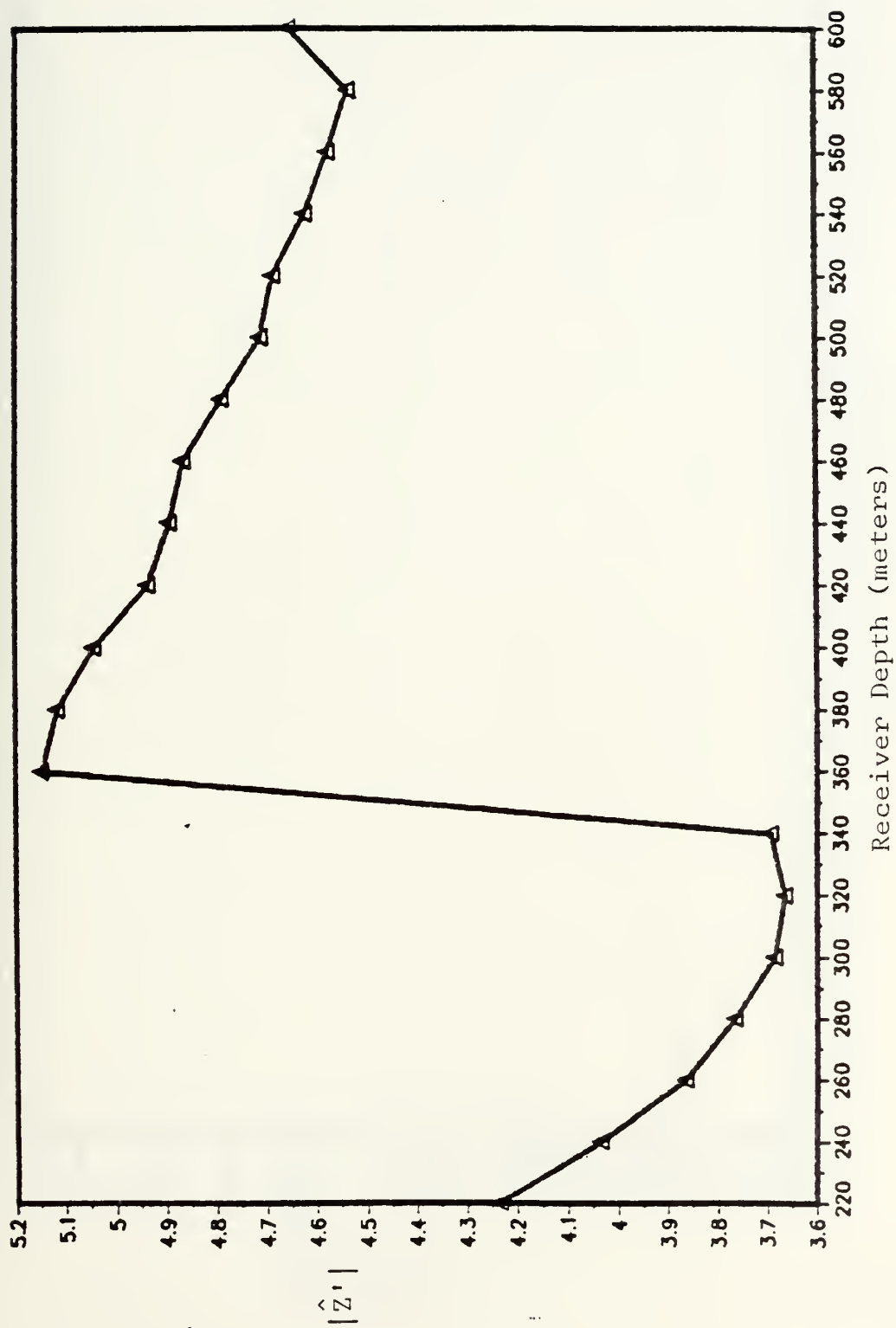


Figure 4.11 Conventional Beam Pattern (non-unity amp. wts. source at 380 m)

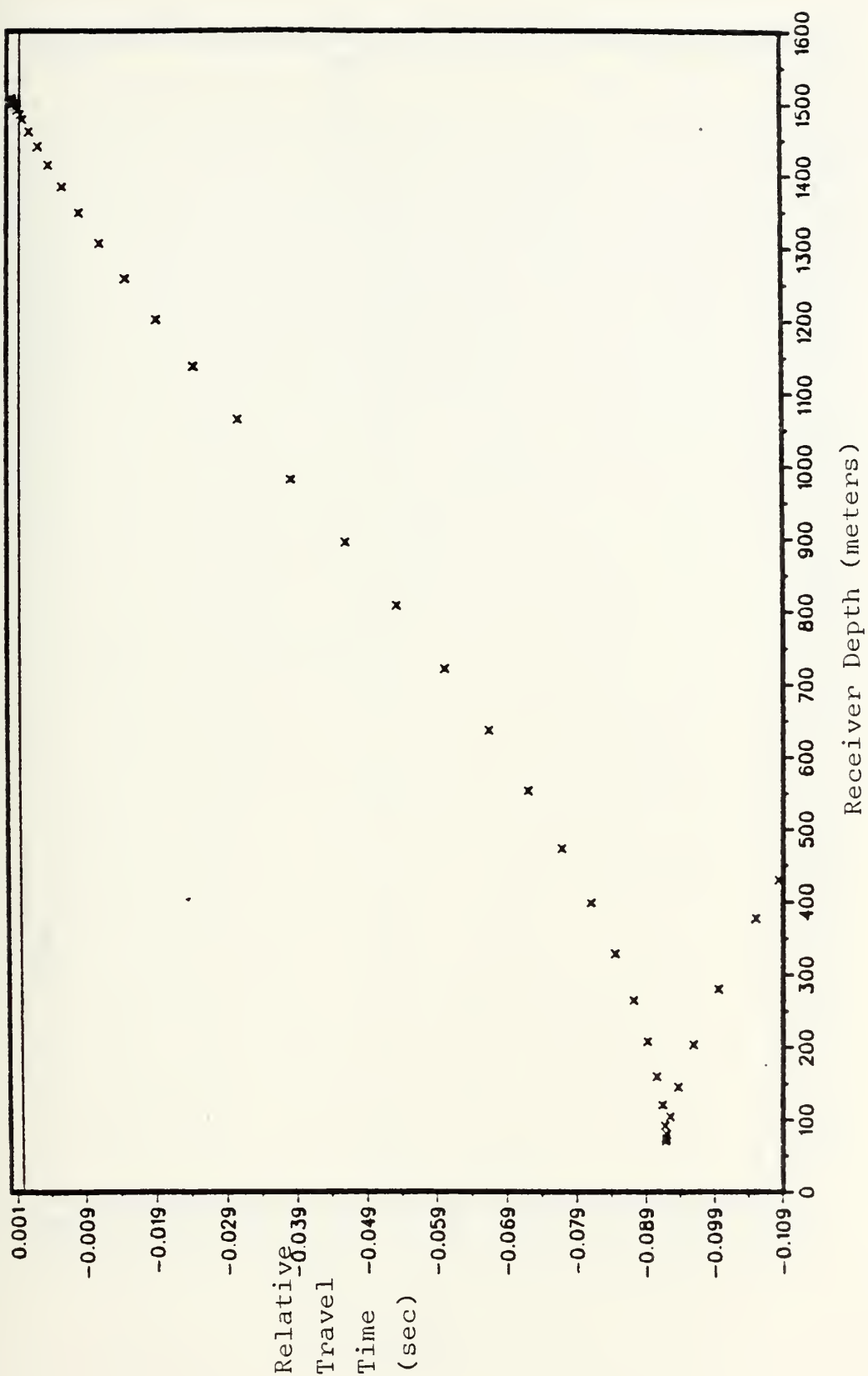


Figure 4.12 Relative Travel Time vs. Depth (range=250 km, source at 220 m)

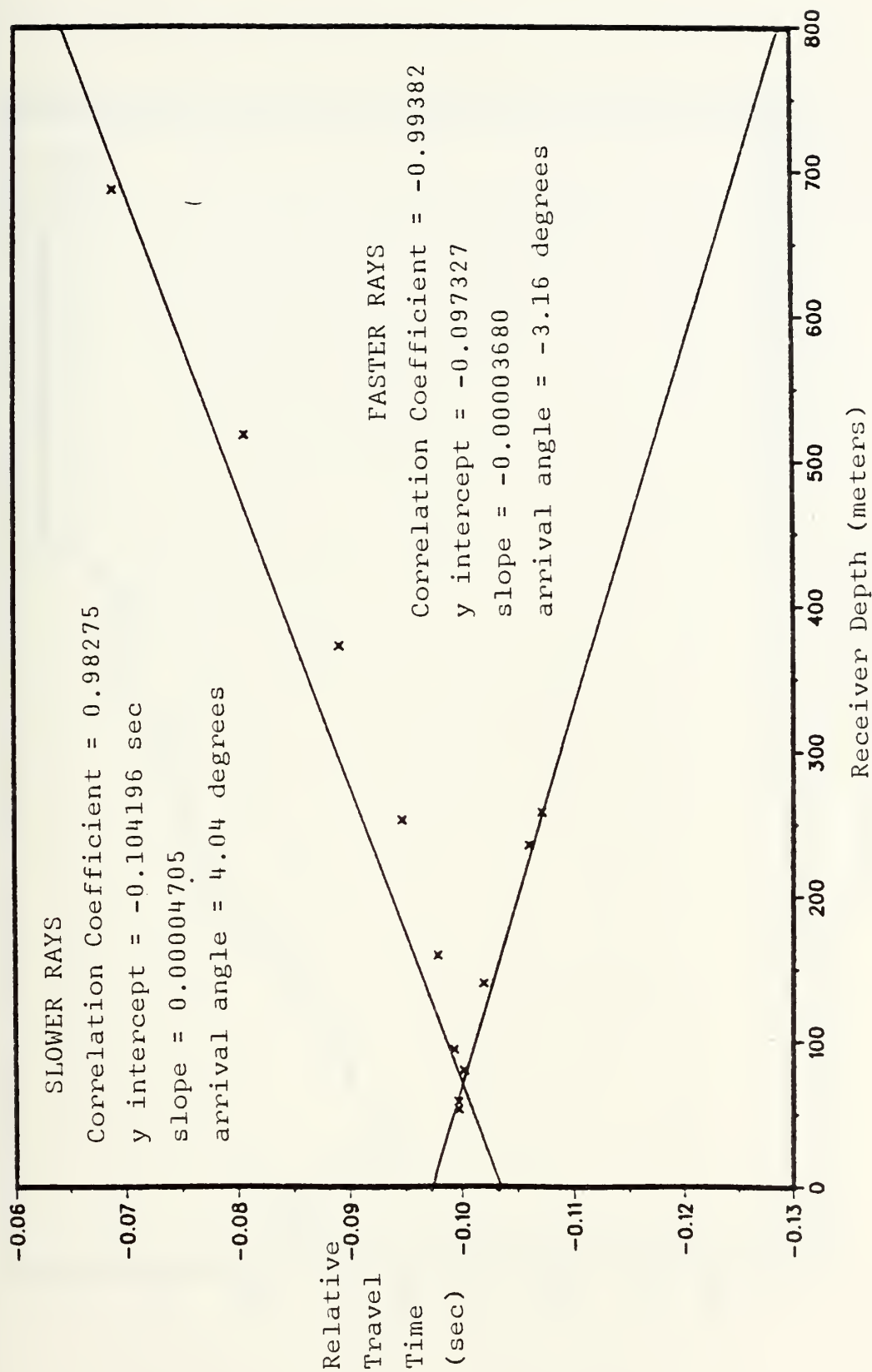


Figure 4.14 St. Line Approx. of Rel. Trav. Time vs. Depth (R=250 km, d=380 m)

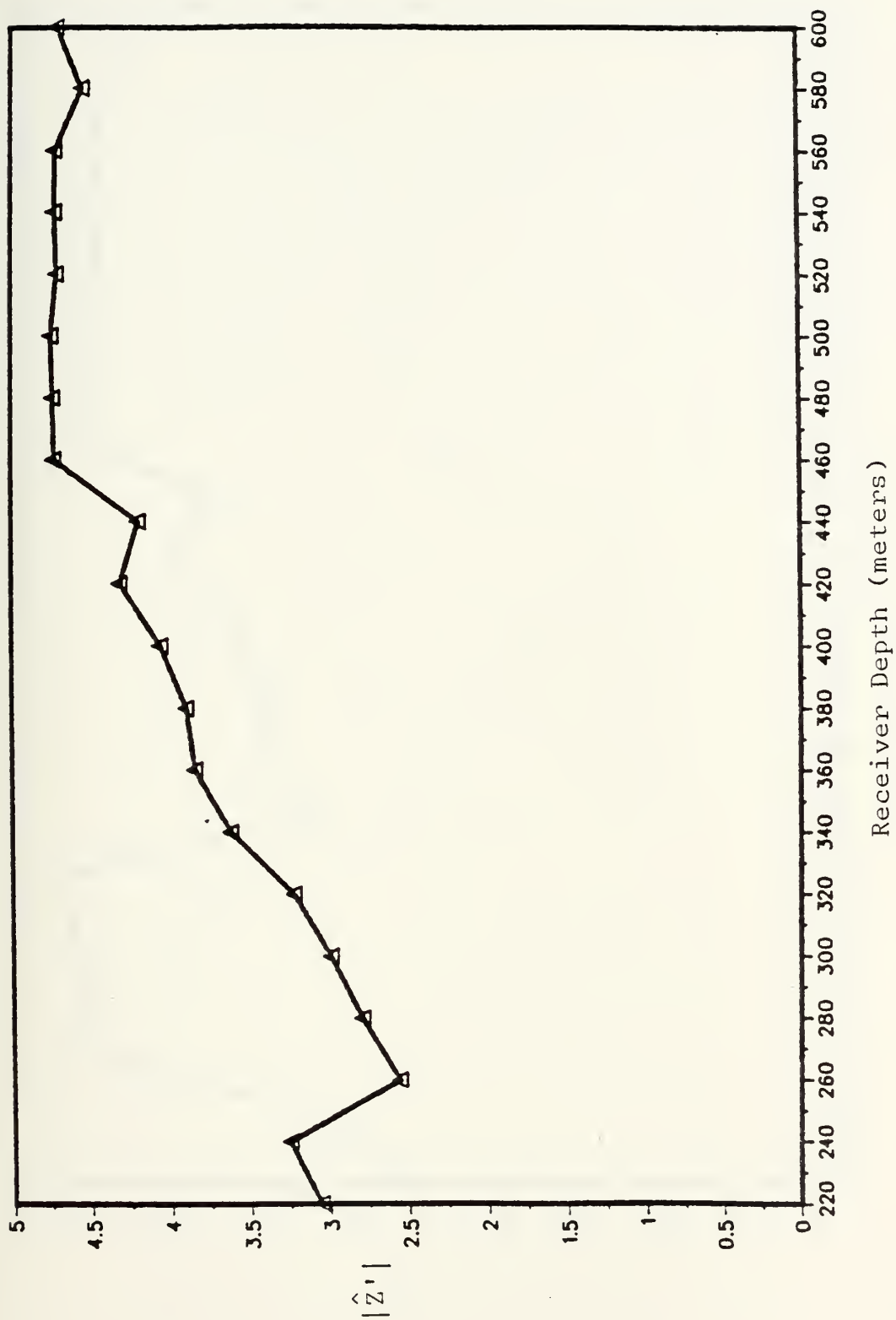


Figure 4.15 Conventional Beam Pattern ($R=250$ km, $d=380$ m, slower times, $a=1$)

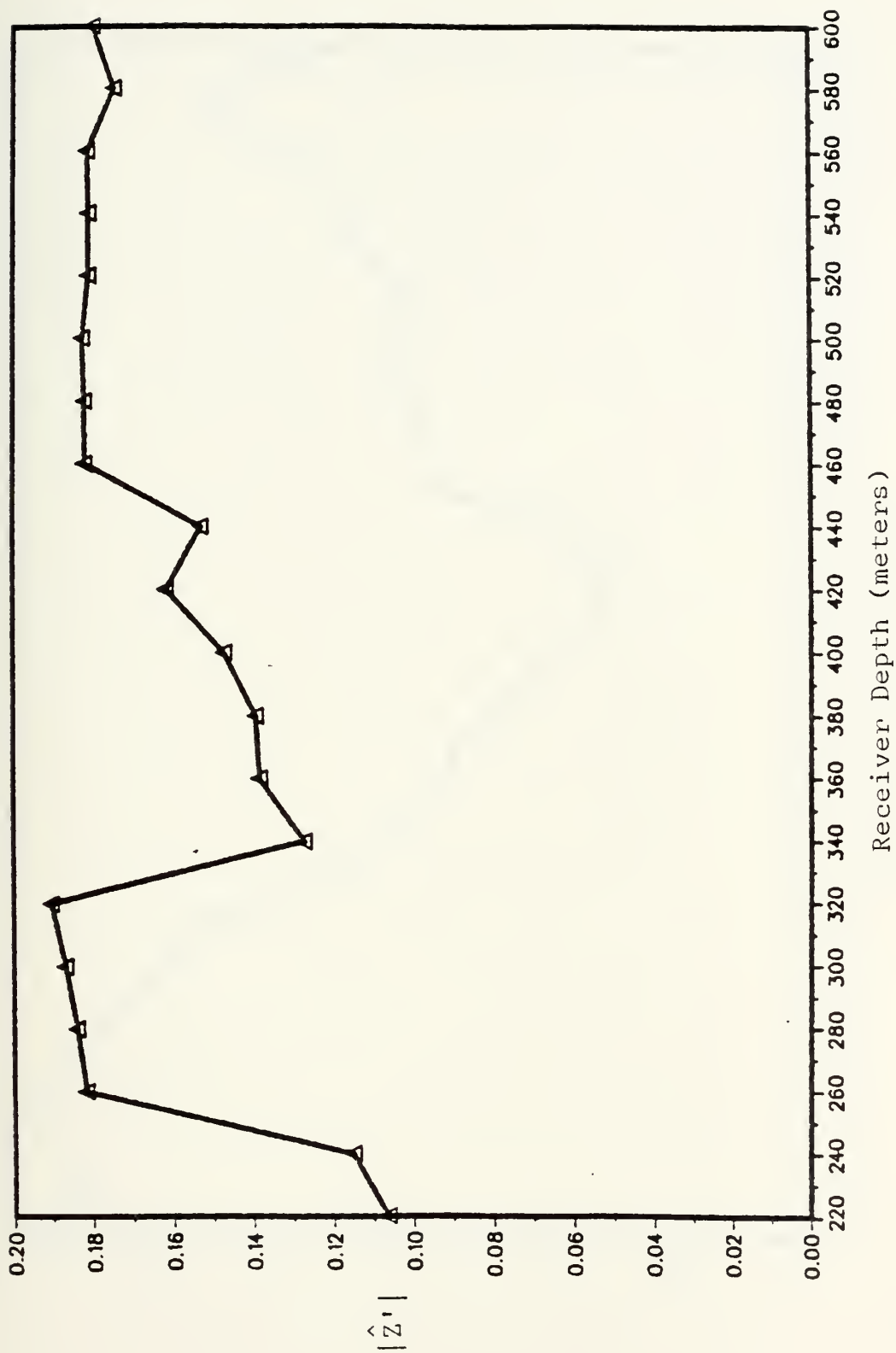


Figure 4.16 Conventional Beam Pattern ($R=250$ km, $d=380$ m, slower times, LMV a)

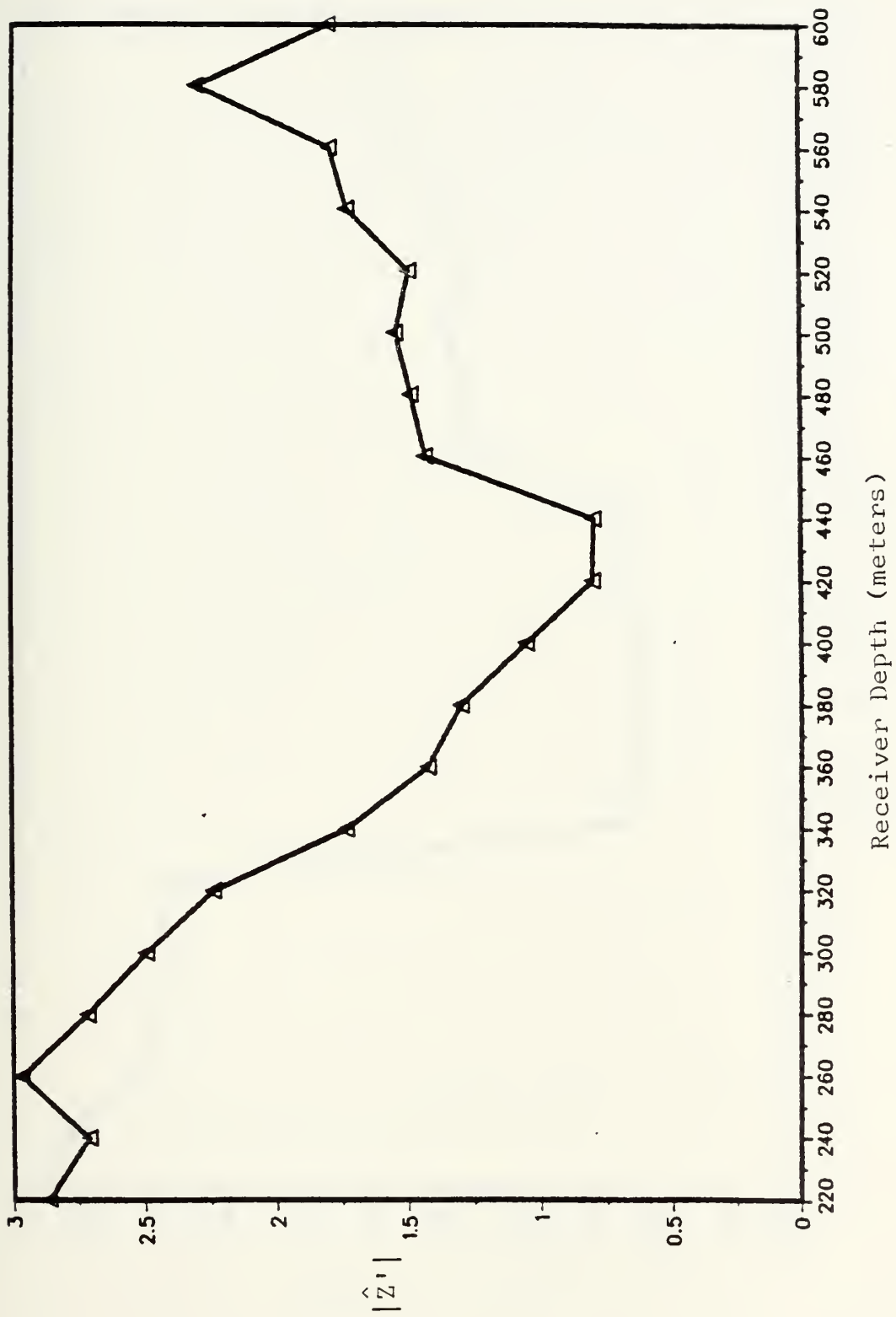


Figure 4.17 Conventional Beam Pattern ($R=250$ km, $d=380$ m, faster times, $a=1$)

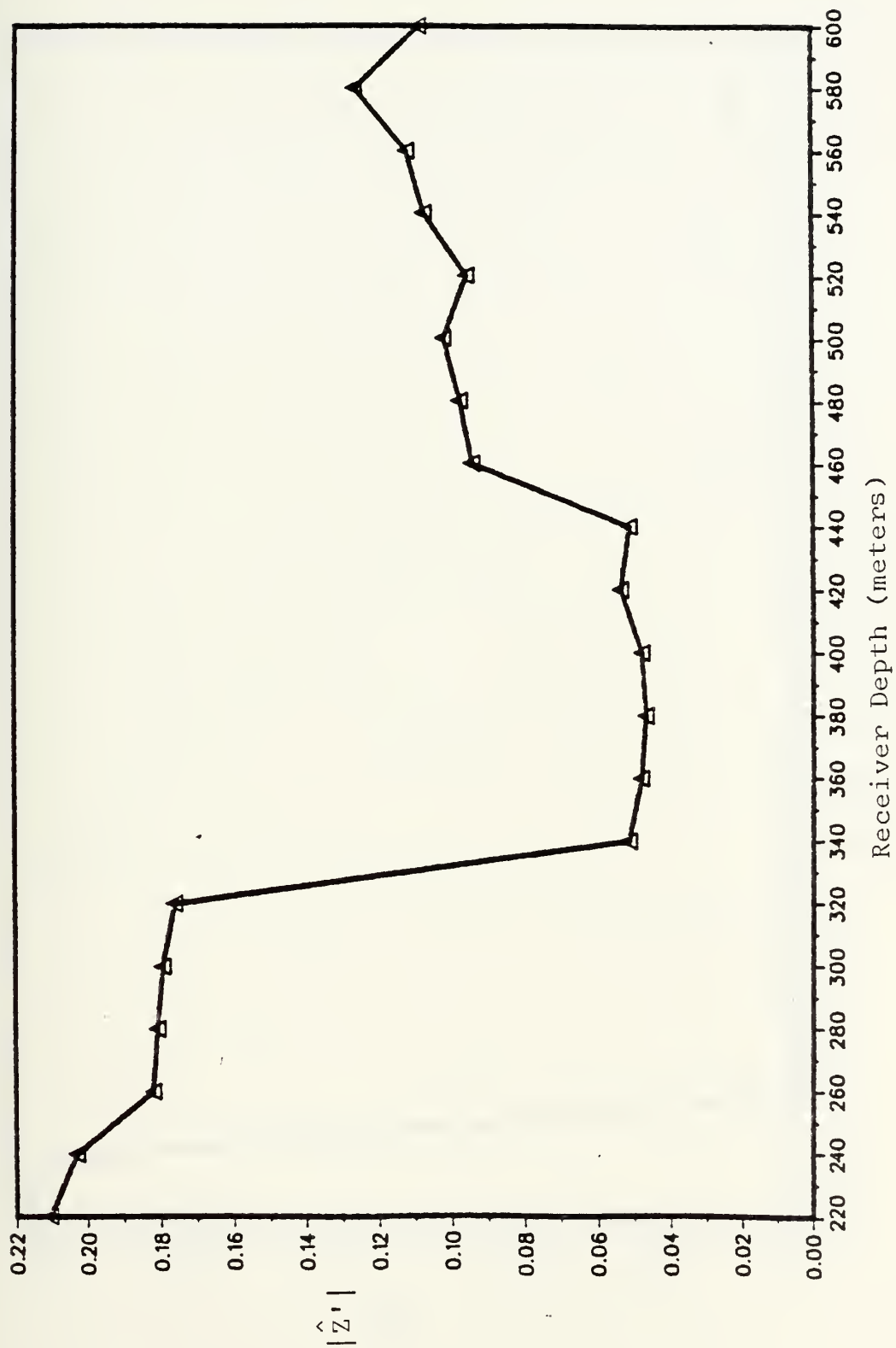


Figure 4.18 Conventional Beam Pattern ($R=250$ km, $d=380$ m, faster times, LMV a)

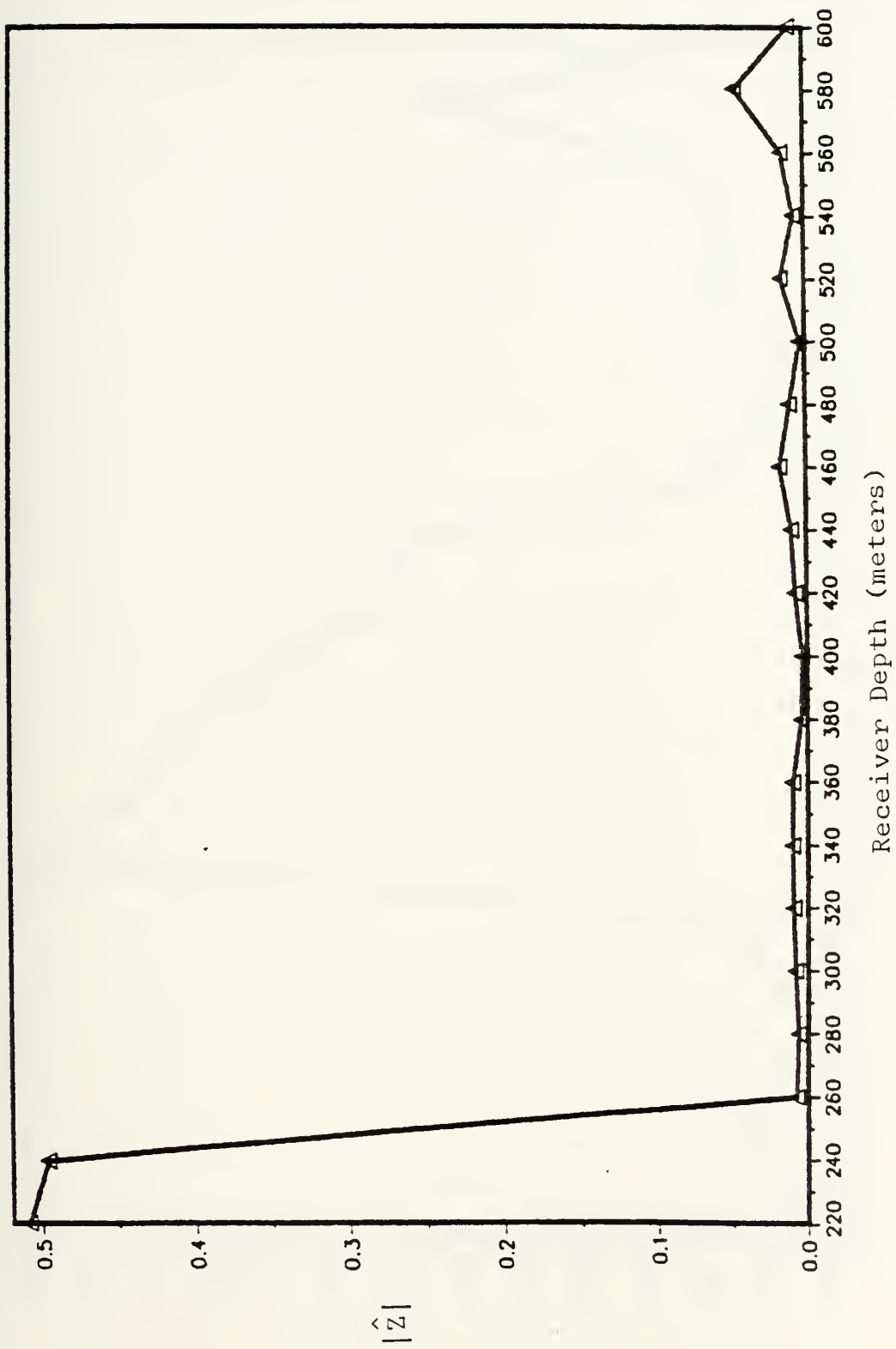


Figure 4.19 Beam Pattern ($R=250$ km, 20 depths, 5 receivers, source at 220 m)

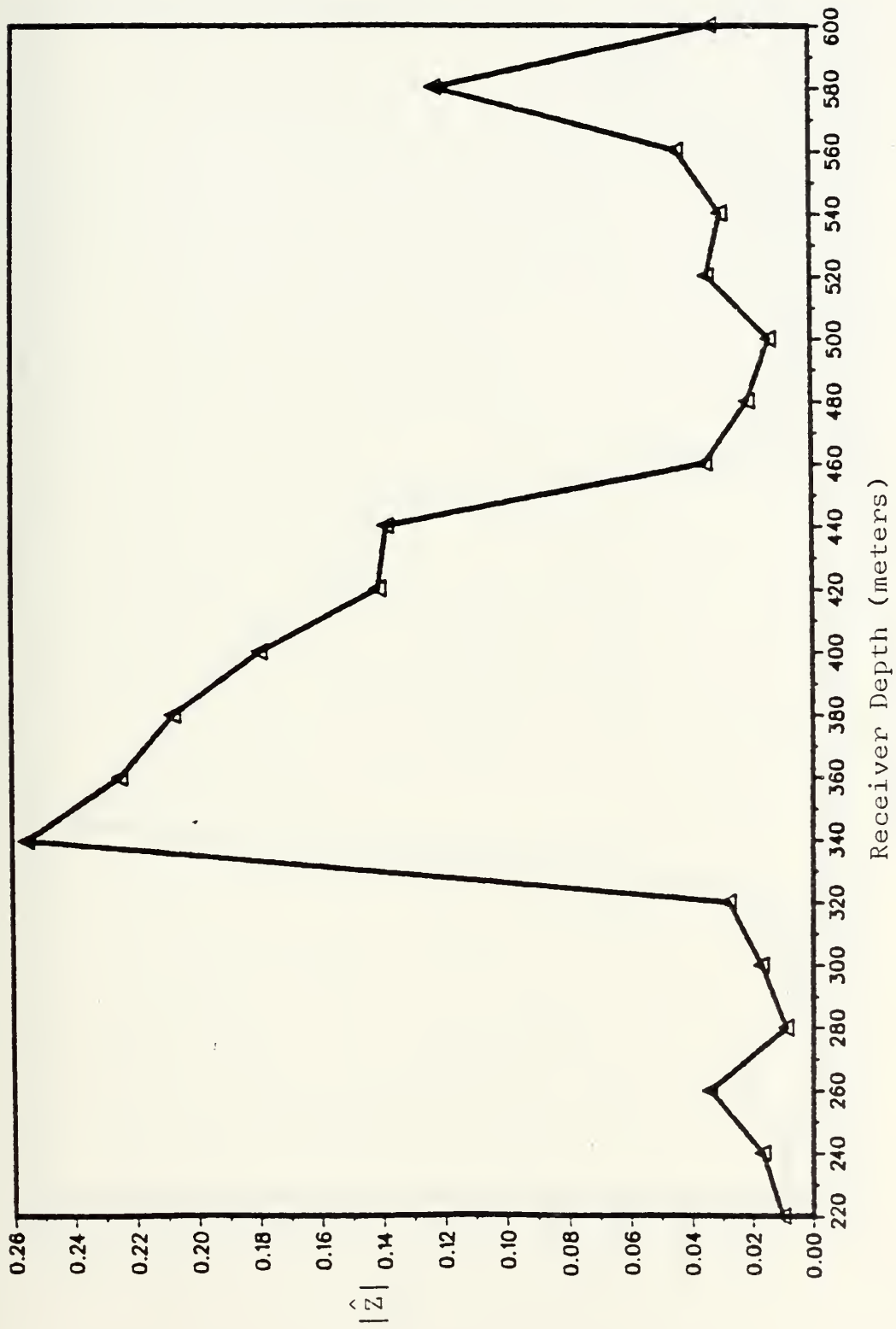


Figure 4.20 Beam Pattern ($R=250$ km, 20 depths, 5 receivers, source at 340 m)

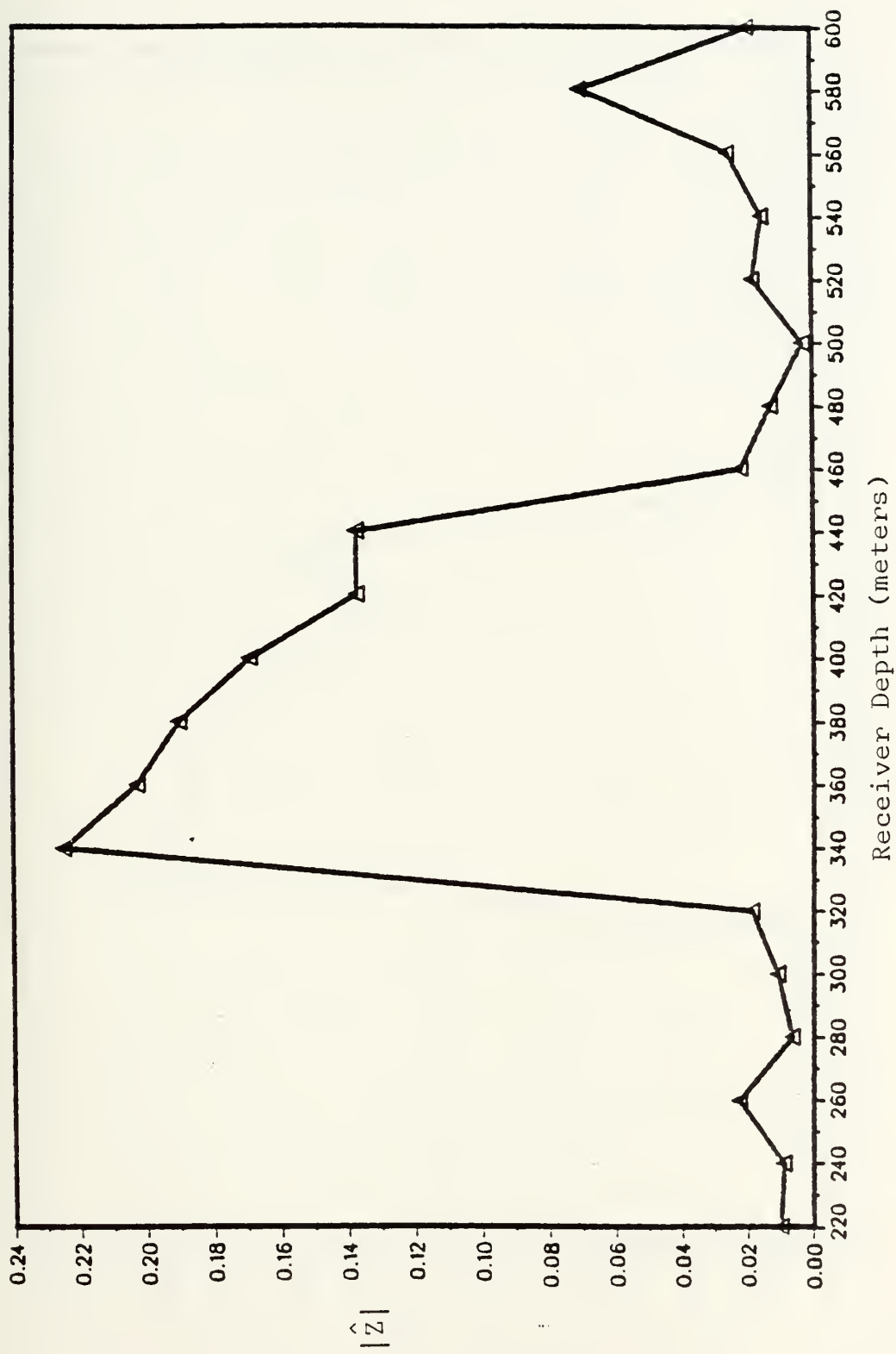


Figure 4.21 Beam Pattern ($R=250$ km, 20 depths, 5 receivers, source at 360 m)

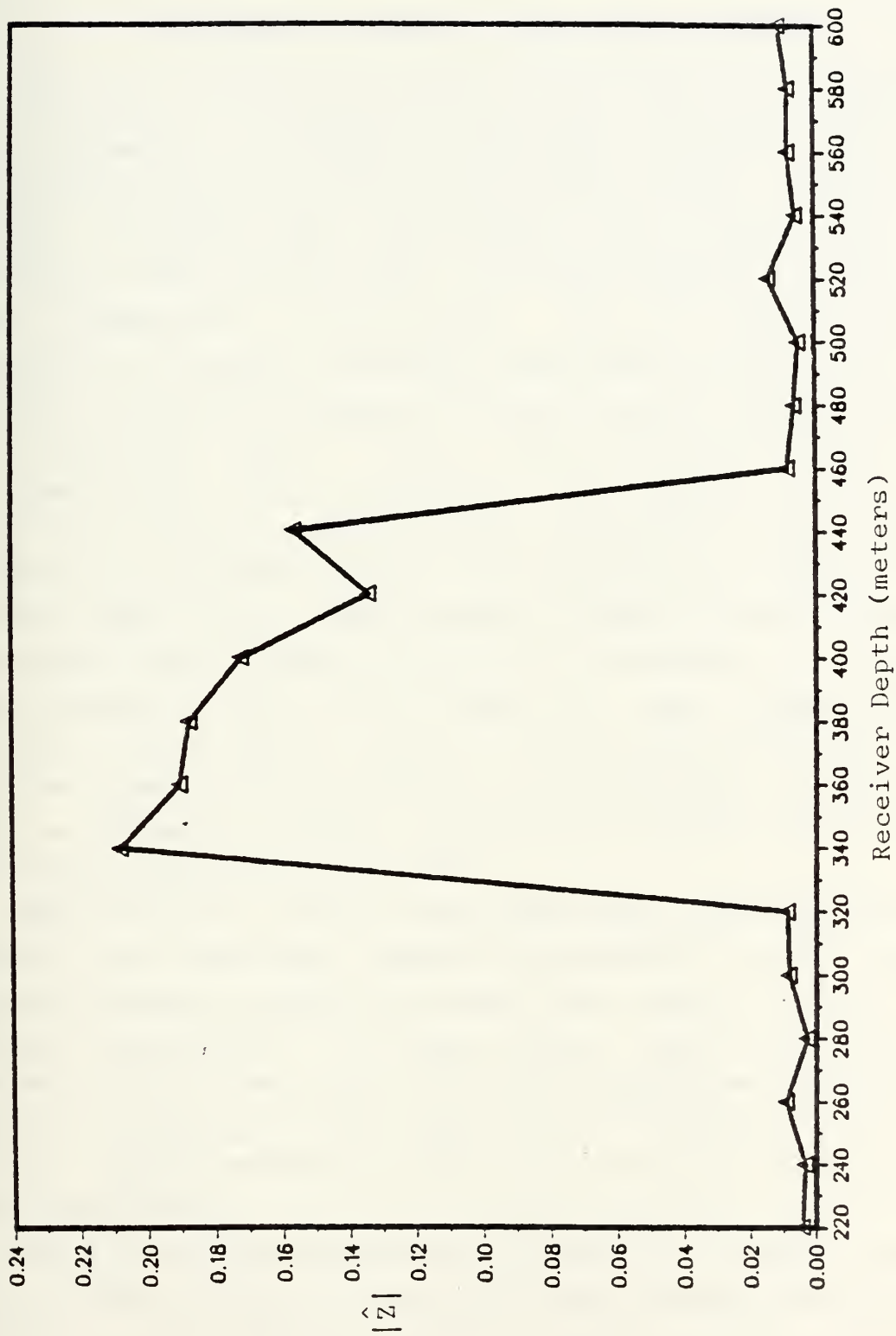


Figure 4.22 Beam Pattern (R=250 km, 20 depths, 5 receivers, source at 380 m)

V. DISCUSSION OF RESULTS AND RECOMMENDATIONS

For many of the cases examined, the linear minimum variance estimation technique gives high resolution in the "depth beam pattern" for sources at long range. Figures 4.2 and 4.3 represent beam patterns for four depths with two receivers where the main lobe is at the desired source depth with a beamwidth of 30 meters. For 20 depths with 2 receivers the system is highly overdetermined and the beam pattern portrayed in figure 4.4 has its main lobe 80 meters from the source depth. At the source depth the strength of the beam pattern is 3.6 db down. For figure 4.5 the main lobe is on the source depth with a beamwidth of 250 meters.

For all 20 source depths with 5 hydrophone receivers the results range from a beam pattern having its main lobe on the source depth (figure 4.7) with a beamwidth of 20 meters and a secondary lobe 12.1 db down to a beam pattern having its main lobe 40 meters from the source depth (figure 4.22). For the beam pattern in figure 4.22 the width of the main lobe is 80 meters and the strength of the beam pattern at the source depth is 0.8 db down.

When using the conventional beamformer, the beam pattern results with amplitude weights determined by the linear minimum variance estimation method were superior to the beam pattern determined by using unity amplitude weights. However in all cases the conventional beamformer was significantly inferior to the beam pattern determined by the linear minimum variance estimation technique in terms of depth resolution.

The linear minimum variance estimation technique could not be used for all ranges with the chosen sound speed profile. For ranges of 187 km and 235 km the relative

travel times produce an 'A' matrix which is so ill-conditioned that the 'IMSL' subroutine 'LINV2F' cannot determine an accurate inverse of 'A^TA'. .

There is sufficient evidence from this initial investigation that the linear minimum variance estimation technique applied to a long linear vertical array can yield high resolution depth information about passive sources at very long ranges. However, further investigation is needed before any field tests are in order. Recommendations for further research are:

1. The use of a more realistic speed of sound profile, preferably one actually characteristic of the 'SCFAR' channel.
2. The use of more hydrophones in the vertical array. As more receivers are used the beam pattern should approach the desired beam pattern more closely (a less overdetermined system should yield smaller total minimum mean square error).
3. Investigation into causes for the peak response falling at other than the desired depth and techniques for correcting this problem when using the linear minimum variance estimation technique.
4. Alternate assumption for choosing the ray paths to include in the 'A' matrix. For example one might choose the rays with the greatest intensity instead of the shortest travel time.
5. The possibility of estimating range as well as the depth of a passive source with linear minimum variance estimation techniques.

In conclusion, the linear minimum variance estimation technique of beamforming was significantly superior to the conventional beamformer. High resolution depth information about passive sources at long ranges is provided.

APPENDIX A
RELATIVE TRAVEL TIME CALCULATION

This program calculates the relative travel times from each source depth to the horizontal range and the depth of the ray at this range. To save paper, only the two shallowest source depths are listed.

THE0C570
THE0C580
THE0C590
THE0C600
THE0C610
THE0C620
THE0C630
THE0C640
THE0C650
THE0C660
THE0C670
THE0C680
THE0C690
THE0C700
THE0C710
THE0C720
THE0C730
THE0C740
THE0C750
THE0C760
THE0C770
THE0C780
THE0C790
THE0C800
THE0C810
THE0C820
THE0C830
THE0C840
THE0C850
THE0C860
THE0C870
THE0C880
THE0C890
THE0C900
THE0C910
THE0C920
THE0C930
THE0C940
THE0C950
THE0C960
THE0C970
THE0C980
THE0C990
THE0C1000
THE0C1010
THE0C1020
THE0C1030
THE0C1040
THE0C1050
THE0C1060
THE0C1070
THE0C1080
THE0C1090
THE0C1100
THE0C1110
THE0C1120
THE0C1130
THE0C1140
THE0C1150
THE0C1160
THE0C1170
THE0C1180
THE0C1190
THE0C1200
THE0C1210
THE0C1220
THE0C1230
THE0C1240
THE0C1250
THE0C1260
THE0C1270
THE0C1280
THE0C1290
THE0C1300
THE0C1310
THE0C1320
THE0C1330
THE0C1340
THE0C1350
THE0C1360
THE0C1370
THE0C1380
THE0C1390
THE0C1400
THE0C1410
THE0C1420
THE0C1430
THE0C1440

```
CRAN=(C1*Y1)/(G*X1)
RAN=RAN+CRAN
R11=RAN
IF (RANGE-RAN)12,12,14
IF HORIZONTAL RANGE OF ARC 1 AND 2 IS LESS THAN THE TOTAL
RANGE THEN CONTINUE PROGRAM, OTHERWISE EXIT TO 12
CALCULATE SUMMED TRAVEL TIME
C1=C1+G*CDEF
DEPTH=DEPTH+CDEP
D2=DEPTH
TIME=TIME+((-1.0C0/G)*DLOG((DTAN(P))/(DTAN(P+(F2/2.0D0))))))
ADD ARC 3
T2=TIME
CDEP=-CDEP
X2=((CDEP*G)/C1)+1.0D0
F2=-DARCSIN(X2)
Y2=DSIN(F2)
DRAN=(C1*(-Y2))/G
RAN=RAN+CRAN
R2=RAN
IF (RANGE-RAN)21,21,22
ADD ARC 4
C1=C1+G*CDEF
DEPTH=DEPTH+CDEP
D3=DEPTH
TIME=TIME+((-1.0C0/G)*DLOG((DTAN(P+(F2/2.0D0))))/(DTAN(P))))
T3=TIME
G=-0.017D0
X1=X2
Y1=Y2
CDEP=(C1*(1.0D0-X1))/(G*X1)
ERAN=C1*Y1/(G*X1)
F1=DARSIN(Y1)
RAN=RAN+ERAN
R3=RAN
IF (RANGE-RAN)41,41,42
ADD ARC 5
C1=C1+G*CDEF
DEPTH=DEPTH+CDEP
```

C
C
C
C
C
14

C
C
C

C
C
C
22

C
C
C
42


```

D4=DEPTH
TIME=TIME+(-1.000/G)*DLOG((DTAN(P))/(DTAN(P+(F1/2.000))))
T4=TIME
CDEP=-CDEP
X2=((CDEP*G)/C1)+1.000
F2=CARCCS(X2)
Y2=DSIN(F2)
FRAN=(C1*(-Y2))/G
RAN=RAN+FRAN
R4=RAN
IF (RANGE-RAN)51,51,52
  ADD ARC 6
C1=C1+G*CDEF
DEPTH=DEPTH+CDEP
D5=DEPTH
TIME=TIME+(-1.000/G)*DLOG((DTAN(P+F2/2.000))/(DTAN(P)))
T5=TIME
X1=X2
Y1=Y2
G=0.01700
CDEP=(C1*(1.000-X1))/(G*X1)
GRAN=(C1*Y1)/(G*X1)
RAN=GRAN+RAN
R5=RAN
IF (RANGE-RAN)61,61,62
  ADD ARC 7
C1=C1+G*CDEF
DEPTH=DEPTH+CDEP
D6=DEPTH
TIME=TIME+(-1.000/G)*DLOG((DTAN(P))/(DTAN(P+(F2/2.000))))
T6=TIME
CDEP=-CDEP
X2=(CDEP*G)/C1+1.000
F2=-DARCCS(X2)
Y2=DSIN(F2)
HRAN=(C1*(-Y2))/G
RAN=RAN+HRAN
R6=RAN
IF (RANGE-RAN)71,71,92
  ADD ARC 8
C1=C1+G*CDEF
DEPTH=DEPTH+CDEP

```

CC52

CC62

CC92

THE01450
THE01460
THE01470
THE01480
THE01490
THE01500
THE01510
THE01520
THE01530
THE01540
THE01550
THE01560
THE01570
THE01580
THE01590
THE01600
THE01610
THE01620
THE01630
THE01640
THE01650
THE01660
THE01670
THE01680
THE01690
THE01700
THE01710
THE01720
THE01730
THE01740
THE01750
THE01760
THE01770
THE01780
THE01790
THE01800
THE01810
THE01820
THE01830
THE01840
THE01850
THE01860
THE01870
THE01880
THE01890
THE01900
THE01910
THE01920


```

D7=DEPTH
TIME=TIME+((-1.0D0/G)*DLOG((DTAN(P)+(F2/2.0D0)))/(DTAN(P)))
T7=TIME
G=-0.017D0
X1=X2
Y1=Y2
CDEP=(C1*(1.0D0-X1))/(G*X1)
RAN1=C1*Y1/(G*X1)
F1=DARSIN(Y1)
RAN=RAN+RAN1
R7=RAN
IF (RANGE-RAN)101,101,102
    ADC ARC 9
C1=C1+G*CDEF
DEPTH=DEPTH+CDEP
D8=DEPTH
TIME=TIME+((-1.0D0/G)*DLOG((DTAN(P))/(DTAN(P)+(F1/2.0D0)))))
T8=TIME
CDEP=-CDEP
X2=((CDEP*G)/C1)+1.0D0
F2=DARCCOS(X2)
Y2=DSIN(F2)
RAN2=(C1*(-Y2))/G
RAN=RAN+RAN2
R8=RAN
IF (RANGE-RAN)111,111,112
    ADC ARC 10
C1=C1+G*CDEF
DEPTH=DEPTH+CDEP
D9=DEPTH
TIME=TIME+((-1.0D0/G)*DLOG((DTAN(P+F2/2.0D0)))/(DTAN(P)))
T9=TIME
X1=X2
Y1=Y2
G=0.017D0
CDEP=(C1*(1.0D0-X1))/(G*X1)
RAN3=(C1*Y1)/(G*X1)
RAN=RAN+RAN3
R9=RAN
IF (RANGE-RAN)121,121,122
    ADC ARC 11
C1=C1+G*CDEF

```

```

THE01930
THE01940
THE01950
THE01960
THE01970
THE01980
THE01990
THE02000
THE02010
THE02020
THE02030
THE02040
THE02050
THE02060
THE02070
THE02080
THE02090
THE02100
THE02110
THE02120
THE02130
THE02140
THE02150
THE02160
THE02170
THE02180
THE02190
THE02200
THE02210
THE02220
THE02230
THE02240
THE02250
THE02260
THE02270
THE02280
THE02290
THE02300
THE02310
THE02320
THE02330
THE02340
THE02350
THE02360
THE02370
THE02380
THE02390
THE02400

```


THE02410
THE02420
THE02430
THE02440
THE02450
THE02460
THE02470
THE02480
THE02490
THE02500
THE02510
THE02520
THE02530
THE02540
THE02550
THE02560
THE02570
THE02580
THE02590
THE02600
THE02610
THE02620
THE02630
THE02640
THE02650
THE02660
THE02670
THE02680
THE02690
THE02700
THE02710
THE02720
THE02730
THE02740
THE02750
THE02760
THE02770
THE02780
THE02790
THE02800
THE02810
THE02820
THE02830
THE02840
THE02850
THE02860
THE02870
THE02880

```

DEPTH=DEPTH+CDEP
D10=DEPTH
TIME=TIME+((-1.0CO/G)*DLOG((DTAN(P))/(DTAN(P+(F2/2.0DO))))))
T10=TIME
CDEP=-CDEP
X2=(CDEP*G)/C1+1.0DO
F2=-DARCS(X2)
Y2=DSIN(F2)
RAN4=(C1*(-Y2))/G
RAN=RAN+RAN4
R6=RAN
IF (RANGE-RAN)131,131,92

CONTINUE ADCING ARCS IF SUMMED HORIZONTAL RANGE IS LESS THAN
TOTAL RANGE, OTHERWISE EXIT TO 131

CALCULATES TRAVEL TIME OF REFERENCE RAY
Y2=Y1-((RANGE-R1A)*G*X1)/C1
F2=DARCSIN(Y2)
X2=DCOS(F2)
CDEP=C1*(X2-X1)/(G*X1)
DEPTH=DEPTH+CDEP
IF (TIME)7,7,8
TIME=(-1.0DC/G)*DLOG((DTAN(P+(F2/2.0DO)))/(DTAN(P)))+TIME
GO TO 32
TIME=(-1.0DC/G)*DLOG((DTAN(P+(F2/2.0DO)))/(CTAN(P+(A1/2.0DO))))
DEGRE=A1*18C.0DO/PI
N=N+1
IF (A1)72,29,72
K1=K1-1
IF (K1)72,811,72
REFTI=TIME
GO TO 72

SUBROUTINE TO CALCULATE DEPTH AND TIME IF HCRIZONTAL RANGE OF
ARC 1 IS GREATER THAN SOURCE-RECEIVER RANGE
F1=F2
Y2=Y1-((RANGE-R1)*G*X1)/C1
F2=DARCSIN(Y2)
X2=DCOS(F2)
CDEP=C1*(X2-X1)/(G*X1)
TIME=T1+((-1.0DO/G)*DLOG((DTAN(P+(F2/2.0DO)))/(DTAN(P+(F1/2.0DO))))
DEPTH=C1+CDEP
GO TO 32

```


SUBROUTINE TO CALCULATE DEPTH AND TIME IF ADDITION OF RANGE OF
ARC 2 CAUSES SUMMED RANGE TO BE GREATER THAN SOURCE-RECEIVER
RANGE

Y2=-(RANGE-R11)*G/C1
F2=DARSIN(Y2)
X2=DCOS(F2)
CDEP=C1*(X2-1.0C0)/G
TIME=T2+(-1.0D0/G)*DLOG((DTAN(P+(F2/2.0D0)))/DTAN(P))
DEPTH=C2+CDEP
GO TO 32

USE IF ARC 3 CAUSES OVERFLOW

Y2=Y1-((RANGE-R2)*G*X1)/C1
F2=DARSIN(Y2)
X2=DCOS(F2)
CDEP=C1*(X2-X1)/(G*X1)
TIME=T3+(-1.0D0/G)*DLOG((DTAN(P+(F2/2.0D0)))/DTAN(P+(F1/2.0D0)))
DEPTH=C3+CDEP
GO TO 32

USE IF ARC 4 CAUSES OVERFLOW

Y2=-(RANGE-R3)*G/C1
F2=DARSIN(Y2)
X2=DCOS(F2)
CDEP=C1*(X2-1.0D0)/G
TIME=T4+(-1.0D0/G)*DLOG((DTAN(P+(F2/2.0D0)))/DTAN(P))
DEPTH=D4+CDEP
GO TO 32

USE IF ARC 5 CAUSES OVERFLOW

F1=F2
Y2=Y1-((RANGE-R4)*G*X1)/C1
F2=DARSIN(Y2)
X2=DCOS(F2)
CDEP=C1*(X2-X1)/(G*X1)
TIME=T5+(-1.0D0/G)*DLOG((DTAN(P+(F2/2.0D0)))/DTAN(P+(F1/2.0D0)))
DEPTH=C5+CDEP
GO TO 32

USE IF ARC 6 CAUSES OVERFLOW

Y2=-(RANGE-R5)*G/C1
F2=DARSIN(Y2)
X2=DCOS(F2)

THE02890
THE02900
THE02910
THE02920
THE02930
THE02940
THE02950
THE02960
THE02970
THE02980
THE02990
THE03000
THE03010
THE03020
THE03030
THE03040
THE03050
THE03060
THE03070
THE03080
THE03090
THE03100
THE03110
THE03120
THE03130
THE03140
THE03150
THE03160
THE03170
THE03180
THE03190
THE03200
THE03210
THE03220
THE03230
THE03240
THE03250
THE03260
THE03270
THE03280
THE03290
THE03300
THE03310
THE03320
THE03330
THE03340
THE03350
THE03360


```

CDEP=C1*(X2-1.0D0)/G
TIME=T6+((-1.0D0/G)*DLOG((DTAN(P+(F2/2.0D0)))/DTAN(P)))
DEPTH=D6+CDEP
GO TO 32

C
C
C 101
USE IF ARC 7 CAUSES OVERFLOW
Y2=Y1-((RANGE-R6)*G*X1)/C1
F2=DARSIN(Y2)
X2=CCOS(F2)
CDEP=C1*(X2-X1)/(G*X1)
TIME=T7+((-1.0D0/G)*DLOG((DTAN(P+(F2/2.0D0)))/DTAN(P+(F1/2.0D0))))
DEPTH=D7+CDEP
GO TO 32

C
C
C 111
USE IF ARC 8 CAUSES OVERFLOW
Y2=-(RANGE-F7)*G/C1
F2=DARSIN(Y2)
X2=CCOS(F2)
CDEP=C1*(X2-1.0D0)/G
TIME=T8+((-1.0D0/G)*DLOG((DTAN(P+(F2/2.0D0)))/DTAN(P)))
DEPTH=D8+CDEP
GO TO 32

C
C
C 121
USE IF ARC 9 CAUSES OVERFLOW
F1=F2
Y2=Y1-((RANGE-R8)*G*X1)/C1
F2=DARSIN(Y2)
X2=CCOS(F2)
CDEP=C1*(X2-X1)/(G*X1)
TIME=T9+((-1.0D0/G)*DLOG((DTAN(P+(F2/2.0D0)))/DTAN(P+(F1/2.0D0))))
DEPTH=D9+CDEP
GO TO 32

C
C
C 131
USE IF ARC 10 CAUSES OVERFLOW
Y2=-(RANGE-F9)*G/C1
F2=DARSIN(Y2)
X2=CCOS(F2)
CDEP=C1*(X2-1.0D0)/G
TIME=T10+((-1.0D0/G)*DLOG((DTAN(P+(F2/2.0D0)))/DTAN(P)))
DEPTH=D10+CDEP
GO TO 32

C
C
C
DEPTH, RELATIVE TIME, AND INITIAL DEPRESSION ANGLE OF RAY ARE
PUT IN A LISTING

```

THE03370
THE03380
THE03390
THE03400
THE03410
THE03420
THE03430
THE03440
THE03450
THE03460
THE03470
THE03480
THE03490
THE03500
THE03510
THE03520
THE03530
THE03540
THE03550
THE03560
THE03570
THE03580
THE03590
THE03600
THE03610
THE03620
THE03630
THE03640
THE03650
THE03660
THE03670
THE03680
THE03690
THE03700
THE03710
THE03720
THE03730
THE03740
THE03750
THE03760
THE03770
THE03780
THE03790
THE03800
THE03810
THE03820
THE03830
THE03840

72

```

K=K+1 TIME=REFTI
Y(K)=DEPTH
X(K)=DEPT
WRITE(6,501)X(K),Y(K),DEGRE
WRITE(8,501)X(K),Y(K),DEGRE
FORMAT(F10.4,F14.7,9X,F12.8)

```

901

```

INCREMENT THE INITIAL DEPRESSION ANGLE BY 0.1 DEGREES AND RESET
INITIAL CONDITIONS. REPEAT THE OPERATION UNTIL MAXIMUM R-R RAY
INITIAL DEPRESSION ANGLE IS REACHED. LAST RAY FROM SOURCE DEPTH
IS AT THIS ANGLE.

```

73

```

IF (A1) 58,73,73
A1=A1+(PI*0.1D0)/180.0D0
RANGE=R
DEPTH=C
CI=C
RAN=0.0C0
TIME=0.0C0
Y1=DSIN(A1)
X1=DCOS(A1)
IF (A1+F3) 88,88,57
I=I+1
A1=-F3
Y1=DSIN(A1)
X1=DCOS(A1)
IF (I-2) 48,55,99

```

97

```

THE FOLLOWING SUBROUTINE IS FOR NEGATIVE (UPWARD) INITIAL
DEPRESSION ANGLES

```

96

```

A1=ANGLE
RANGE=R
DEPTH=C
CI=C
A1=A1-(PI*0.1D0)/180.0D0
Y1=DSIN(A1)
X1=DCOS(A1)
IF (A1+(-F3)) 93,53,53
I=I+1
A1=F3
Y1=DSIN(A1)
X1=DCOS(A1)
IF (I-4) 53,95,99
G=-0.017D0
R1A=CI*Y1/(C*X1)

```

93

53

```

THE03850
THE03860
THE03870
THE03880
THE03890
THE03900
THE03910
THE03920
THE03930
THE03940
THE03950
THE03960
THE03970
THE03980
THE03990
THE04000
THE04010
THE04020
THE04030
THE04040
THE04050
THE04060
THE04070
THE04080
THE04090
THE04100
THE04110
THE04120
THE04130
THE04140
THE04150
THE04160
THE04170
THE04180
THE04190
THE04200
THE04210
THE04220
THE04230
THE04240
THE04250
THE04260
THE04270
THE04280
THE04290
THE04300
THE04310
THE04320

```



```

82      IF (RANGE-R1)/81,81,82
      CDEP=C1*(1.00-X1)/(G*X1)
      RAN=R1A
      TIME=(-1.00(G/G)*DLOG((DTAN(P))/DTAN(P+(A1/2.000))))
      X1=1.00C
      Y1=0.00C
      DEPTH=CDEP+LEP TH
      C1=C1+G*CDEF
      GO TO 88
81      Y2=Y1-(RANGE*G*X1)/C1
      F2=DARSIN(Y2)
      X2=DCOS(F2)
      TIME=(-1.00(G/G)*DLOG((DTAN(P+(F2/2.000)))/DTAN(P+(A1/2.000))))
      CDEP=C1*(X2-X1)/(G*X1)
      DEPTH=DEPTH+CDEP
      GO TO 32
      K IS THE NUMBER OF RAYS CALCULATED FOR EACH SOURCE DEPTH
      CONTINUE
      WRITE(6,991)DEPTH,K
      WRITE(8,991)DEPTH,K
      FORMAT(IX,NUMBER OF RAYS FOR THE ',F7.2,' METER DEPTH IS',IX,13)
178      WRITE(6,178)
531      WRITE(8,178)
      FORMAT(IX,')
      CONTINUE
      INCREMENT THE SOURCE DEPTH 20 METERS UNTIL 600 METERS
      IS EXCEEDED
      IF (DEPTH-600.000)5,9,9
      CONTINUE
      STOP
      END
      DEPTH      RELATIVE TRAVEL TIME      INITIAL ANGLE
1157.4079      0.0012725      0.0000000
1173.6307      0.0022367      0.1000000
1185.6802      0.0028523      0.2000000
1193.6744      0.0031453      0.3000000
1197.7002      0.0031655      0.4000000
1197.8063      0.0031606      0.5000000
1193.9812      0.0022450      0.6000000
1186.1832      0.0013153      0.7000000
1174.3260      0.0000505      0.8000000
1158.2750      -0.0016306      0.9000000
1137.8606      0.0000000      1.0000000

```


NUMBER OF	DEPT	RELATIVE	TRAVEL	TIME	220.00	METER DEPTH	IS	42	THE
112	8688	-0.	037000			1	100000000		THE04810
11083	8641	-0.	0622330			1	200000000		THE04820
11048	10123	-0.	0922386			1	300000000		THE04830
11067	3558	-0.	128722			1	400000000		THE04840
10962	3846	-0.	169717			1	500000000		THE04850
913	8616	-0.	212090			1	600000000		THE04860
862	6216	-0.	255669			1	700000000		THE04870
805	0437	-0.	299738			1	800000000		THE04880
753	5937	-0.	343231			1	900000000		THE04890
638	7140	-0.	386434			2	100000000		THE04900
638	9217	-0.	427604			2	200000000		THE04910
580	6477	-0.	467310			2	300000000		THE04920
522	2753	-0.	504554			2	400000000		THE04930
465	6422	-0.	538628			2	500000000		THE04940
405	1722	-0.	569386			2	600000000		THE04950
354	9462	-0.	596485			2	700000000		THE04960
305	2015	-0.	620132			2	800000000		THE04970
254	5738	-0.	639836			2	900000000		THE04980
165	2658	-0.	655253			3	100000000		THE04990
133	3508	-0.	667447			3	200000000		THE05000
104	3208	-0.	675970			3	300000000		THE05010
81	3518	-0.	680558			3	400000000		THE05020
65	3323	-0.	683573			3	500000000		THE05030
57	3071	-0.	684673			3	600000000		THE05040
57	9020	-0.	684959			3	700000000		THE05050
67	8515	-0.	685065			3	800000000		THE05060
87	8950	-0.	686560			3	900000000		THE05070
118	7971	-0.	690506			3	100000000		THE05080
161	3067	-0.	699827			4	200000000		THE05090
185	4389	-0.	715197			4	300000000		THE05100
185	4389	-0.	725201			4	40685864		THE05110
									THE05120
									THE05130
									THE05140
									THE05150
									THE05160
									THE05170
									THE05180
									THE05190
									THE05200
									THE05210
									THE05220
									THE05230
									THE05240
									THE05250
									THE05260
									THE05270
									THE05280

1305.5720
 11273.11330
 112336.54325
 111332.25275
 110774.42654
 10035.38578
 8682.19706
 714.77504
 641.72507
 565.06417
 432.74477
 368.65722
 308.48118
 252.90885
 202.65075
 158.91756
 120.93398
 90.17225
 65.38338
 53.33088
 36.77598
 19.50299
 7.28025
 1153.8985
 167.9190
 NUMBER CF

0.0111410
 0.0086388
 0.0055768
 0.00199620
 -0.00233034
 -0.00732848
 -0.001327747
 -0.00260831
 -0.00378035
 -0.00431235
 -0.00479999
 -0.00523572
 -0.00566407
 -0.00596466
 -0.00624466
 -0.00664672
 -0.00677407
 -0.00685519
 -0.00690749
 -0.00692636
 -0.00693339
 -0.00693250
 -0.00694228
 -0.00697576
 -0.00706456
 -0.00721825
 -0.00727444
 RAYS FCR THE

240.00 METER DEPTH IS 44

THE05290
 THE05300
 THE05310
 THE05320
 THE05330
 THE05340
 THE05350
 THE05360
 THE05370
 THE05380
 THE05390
 THE05400
 THE05410
 THE05420
 THE05430
 THE05440
 THE05450
 THE05460
 THE05470
 THE05480
 THE05490
 THE05500
 THE05510
 THE05520
 THE05530
 THE05540
 THE05550
 THE05560
 THE05570
 THE05580
 THE05590
 THE05600

APPENDIX B
INTERPOLATION OF RELATIVE TRAVEL TIME CALCULATIONS

This program does an interpolation of the output data generated in Appendix A. The relative travel times are interpolated for the receiving hydrophone depths.


```

C      EVALUATES THE SLICE AT THESE POINTS
C      U(1)=100.0
C      U(2)=200.0
C      U(3)=300.0
C      U(4)=400.0
C      U(5)=500.0
C      CALL ICSEVU(X,Y,NX,C,K1,U,S,5,IER)
C      OUTPUT ARE TRAVEL TIMES PRINTED BY ROW. THE FIRST ROW IS FOR
C      THE SHALLOWEST SOURCE DEPTH AND LAST ROW IS FOR THE DEEPEST
C      SOURCE DEPTH. THE FIRST COLUMN IS FOR THE SHALLOWEST RECEIVING
C      HYDROPHONE AND THE FINAL COLUMN IS FOR THE DEEPEST HYDROPHONE.
C      WRITE(6,101)(S(I),I=1,5)
C      WRITE(7,101)(S(I),I=1,5)
C      FORMAT(5F14.7)
C      PROGRAM TERMINATES WHEN NUMBER OF RAYS FOR A SOURCE DEPTH EQUALS
C      THE NUMBER OF RAYS FOR THE DEEPEST SOURCE DEPTH
C      IF(K(IJ)-68)2,21,21
C      CONTINUE
C      STOP
C      END
21      $ENTRY
-0.0654165-0.0658337-0.0621516-0.0574149-0.0518334
-0.0703212-0.0665503-0.0628172-0.0580503-0.0524011
-0.0713123-0.0673456-0.0635689-0.0587241-0.0530590
-0.0723207-0.0681941-0.0643641-0.0595105-0.0537945
-0.0745428-0.0695940-0.0652127-0.0603237-0.0546137
-0.0756658-0.0709912-0.0670775-0.0621397-0.0563615
-0.0772097-0.0720147-0.0680565-0.0631501-0.0572667
-0.0780555-0.0731056-0.0691335-0.0641502-0.0583075
-0.0795755-0.0742301-0.0701951-0.0652131-0.0593780
-0.0817558-0.0765576-0.0724953-0.0674813-0.0616073
-0.0838838-0.0787900-0.0747091-0.0696366-0.0627376
-0.0851952-0.0803677-0.0764425-0.0711268-0.0639641
-0.0863854-0.0817073-0.0775561-0.0724360-0.0664785
-0.0874630-0.0830759-0.0788332-0.0737404-0.0677993
-0.0885926-0.0844590-0.0802819-0.0751390-0.0691366
-0.0898928-0.0859060-0.0816601-0.0764943-0.0705184
-0.0902551-0.0873991-0.0830757-0.0795512-0.0719424

```


APPENDIX C
RESULTING BEAM PATTERN FOR CALCULATED WEIGHTS

This program uses the output of Appendix B to calculate the 'A' matrix. From this, the amplitude and phase weights are determined by the linear minimum variance estimation technique. These weights are applied to the array and the beam pattern is obtained.


```

999      WRITE(6,999)
        FORMAT(IX,ANS MATRIX (PHASE AND AMPLITUDE WEIGHTS) FOLLOWS.)
158      WRITE(6,158)(ANS(I8,1),I8=1,10)
        FORMAT(F14.7)
C
C      APPLYING THESE PHASE AND AMPLITUDE WEIGHTS, THE RESULTING BEAM
C      PATTERN IS CALCULATED (REAL AND IMAGINARY PARTS SEPARATE)
760      CALL VMLFF(A,ANS, 40,10,1,40,10,Y,40,IER2)
C
C      THE REAL AND IMAGINARY PARTS OF THE RESULTING BEAM PATTERN
C      ARE COMBINED TO GIVE ABSOLUTE VALUE.
987      I20=I20+1
        XX(I20,1)=SQRT(Y(I20,1)*Y(I20,1)+Y(I20+20,1)*Y(I20+20,1))
        IF(I20-20)987,654,654
        I19=I19+1
        X1(I19,1)=2(0.0+I19*20.0
        IF(I19-20)654,655,655
C
C      PRINT SOURCE DEPTH AND ABSOLUTE VALUE OF BEAM PATTERN AT
C      THAT DEPTH
654      WRITE(6,988)(X1(I,1),XX(I,1),I=1,20)
        WRITE(9,988)(X1(I,1),XX(I,1),I=1,20)
988      FORMAT(F8.2,' METER DEPTH HAS STRENGTH CF ',F14.7)
172      CONTINUE
        STOP
$ENTRY
ANS MATRIX (PHASE AND AMPLITUDE WEIGHTS) FOLLOWS
-0.0050524
2.275893C
0.5812412
-3.606538C
-4.330297C
0.2429787
-1.373913C
-3.074544C
2.144663C
C.7122661
MA900570
MA900580
MA900590
MA901000
MA901010
MA901020
MA901030
MA901040
MA901050
MA901060
MA901070
MA901080
MA901090
MA901100
MA901110
MA901120
MA901130
MA901140
MA901150
MA901160
MA901170
MA901180
MA901190
MA901200
MA901210
MA901220
MA901230
MA901240
MA901250
MA901260
MA901270
MA901280
MA901290
MA901300
MA901310
MA901320
MA901330
MA901340
MA901350
MA901360
MA901370
MA901380
MA901390
MA901400
MA901410
MA901420
MA901430
MA901440

```


22	C.	00	ME	TE	DE	HAS	STRENGTH	0.	743061
24	C.	00	ME	TE	DE	HAS	STRENGTH	0.	2850570
26	C.	00	ME	TE	DE	HAS	STRENGTH	0.	2128562
28	C.	00	ME	TE	DE	HAS	STRENGTH	0.	2804181
30	C.	00	ME	TE	DE	HAS	STRENGTH	0.	0716652
32	C.	00	ME	TE	DE	HAS	STRENGTH	0.	0349326
34	C.	00	ME	TE	DE	HAS	STRENGTH	0.	1124682
36	C.	00	ME	TE	DE	HAS	STRENGTH	0.	0530375
38	C.	00	ME	TE	DE	HAS	STRENGTH	0.	0693972
40	C.	00	ME	TE	DE	HAS	STRENGTH	0.	1343069
42	C.	00	ME	TE	DE	HAS	STRENGTH	0.	1722233
44	C.	00	ME	TE	DE	HAS	STRENGTH	0.	1437957
46	C.	00	ME	TE	DE	HAS	STRENGTH	0.	0185341
48	C.	00	ME	TE	DE	HAS	STRENGTH	0.	0239681
50	C.	00	ME	TE	DE	HAS	STRENGTH	0.	0197991
52	C.	00	ME	TE	DE	HAS	STRENGTH	0.	0891870
54	C.	00	ME	TE	DE	HAS	STRENGTH	0.	0190372
56	C.	00	ME	TE	DE	HAS	STRENGTH	0.	1875219
58	C.	00	ME	TE	DE	HAS	STRENGTH	0.	0271981
60	C.	00	ME	TE	DE	HAS	STRENGTH	0.	0740827
MA901450									
MA901460									
MA901470									
MA901480									
MA901490									
MA501500									
MA901510									
MA901520									
MA901530									
MA901540									
MA901550									
MA901560									
MA901570									
MA901580									
MA901590									
MA901600									
MA901610									
MA901620									
MA901630									
MA901640									
MA901650									

LIST OF REFERENCES

1. Officer, C. E., Introduction to the Theory of Sound Transmission, McGraw-Hill, 1958.
2. Kinsler, L. E., and others, Fundamentals of Acoustics, Wiley, 1982.
3. Melsa, J. L. and Cohn, A. B., Decision and Estimation Theory, McGraw-Hill, 1978.

INITIAL DISTRIBUTION LIST

	No. Copies
1. Defense Technical Information Center Cameron Station Alexandria, Virginia 22314	2
2. Library, Code 0142 Naval Postgraduate School Monterey, California 93943	2
3. Department Chairman, Code 62 Department of Electrical Engineering Naval Postgraduate School Monterey, California 93943	1
4. Professor P.H. Mose, Code 62Me Department of Electrical Engineering Naval Postgraduate School Monterey, California 93943	6
5. Professor L.J. Ziomek, Code 62Zm Department of Electrical Engineering Naval Postgraduate School Monterey, California 93943	1
6. Lt (N) D.P. McVicar 33 Hawthorne St. Antigonish, Nova Scotia B2G 1A2 Canada	4
7. EMCS-3 National Defence Headquarters Ottawa, Ontario K1A 0K2 Canada	4
8. DPED National Defence Headquarters Ottawa, Ontario K1A 0K2 Canada	2
9. Captain D. Cantley 4073 El Bosque Pebble Beach, California 93953	1

207507

Thesis

M272 McVicar

c.1 Amplitude shading
 and phase weighting of
 a vertical linear array
 in the SOFAR channel by
 the linear minimum var-
 iance estimation tech-
 nique.

207507

Thesis

M272 McVicar

c.1 Amplitude shading
 and phase weighting of
 a vertical linear array
 in the SOFAR channel by
 the linear minimum var-
 iance estimation tech-
 nique.



thesM272

Amplitude shading and phase weighting of



3 2768 002 03372 2

DUDLEY KNOX LIBRARY